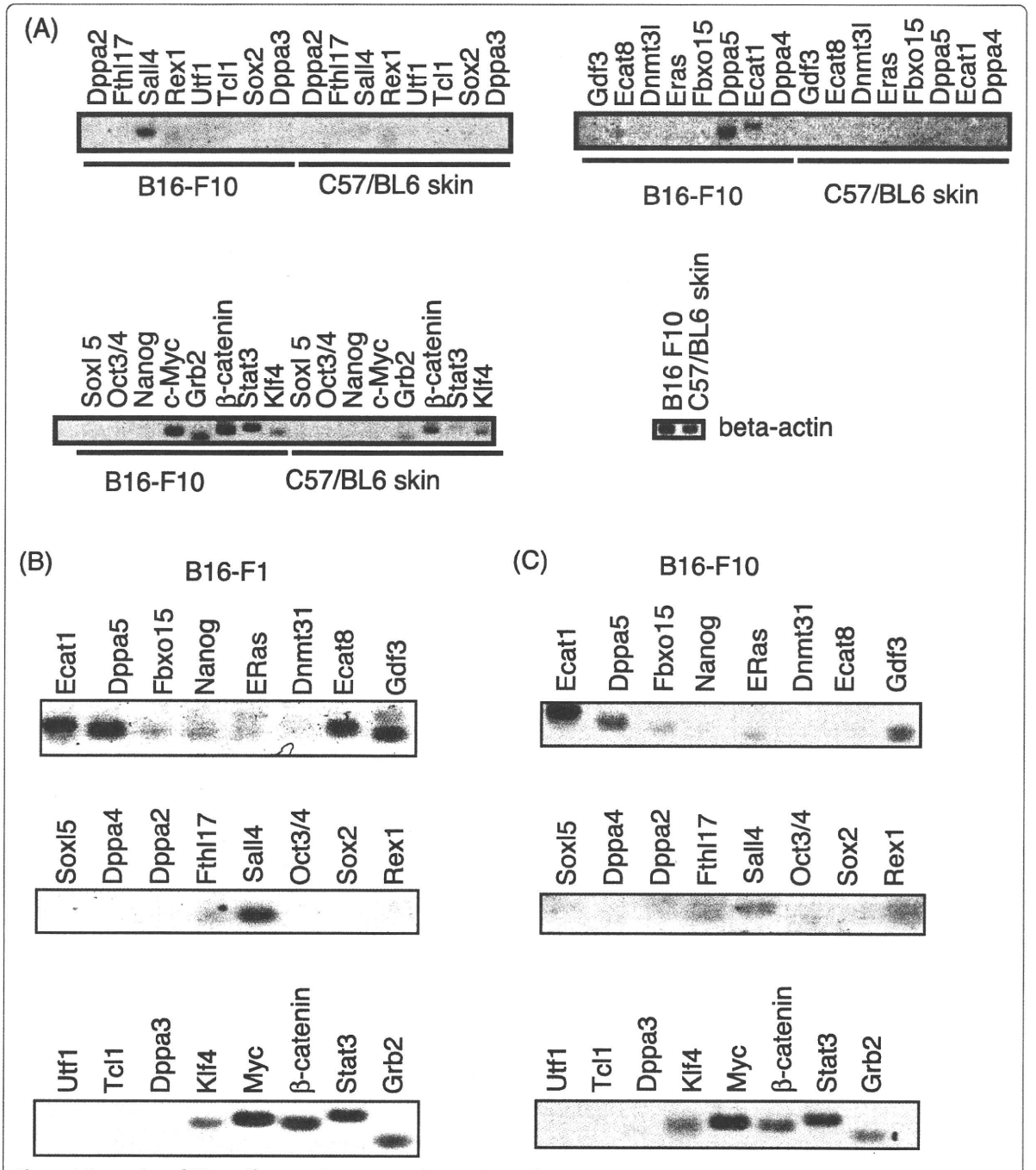

Figure 1 Expression of ES-specific genes in mouse melanoma B16 cells. (A) Total RNA was extracted from B16-F10 cells cultured in 10-cm dishes and RT-PCR was performed with primers listed in Table 1. Total RNA from excised C57BL/6 mice skin was used as control. B16-F10 cells expressed mRNA of Sall4, Dppa5, Ecat1, c-Myc, Grb2, β-catenin, and Stat3, which were not expressed in control C57/BL6 skin samples. (B, C) B16-F1 (B) or B16-F10 cells (C) were injected subcutaneously into C57BL/6 mice. Seven days after the injection, the tumor was excised. Total RNA was extracted and RT-PCR was performed. Two additional experiments resulted in similar profiles to that shown here.

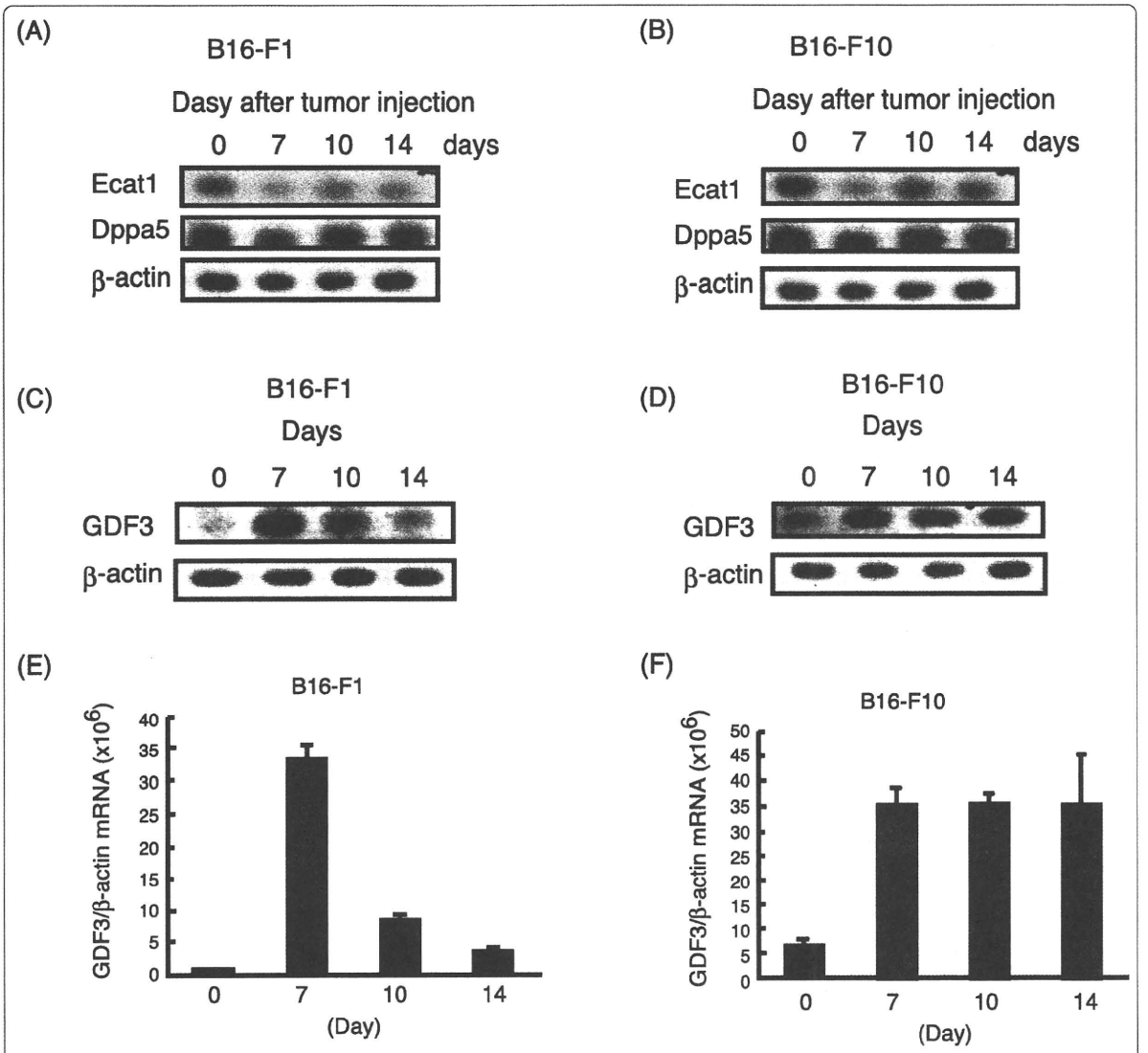

Figure 2 Expression kinetics of Ecat1, Dppa5, and GDF3 during tumorigenesis. B16-F1 and B16-F10 cells were injected subcutaneously into C57BL/6 mice. Tumors were excised on the indicated day. Total RNA was extracted from the tumor and RT-PCR (A-D) or RT-qPCR (E, F) was performed to detect Ecat1, Dppa5, and GDF3. (A, B) RT-PCR analyses revealed that mRNA of Eca1 and Dppa5 decreased during tumorigenesis. (C, E) In B16-F1 cells, GDF3 peaked at day 7 after tumor injection and then gradually decreased. (D, F). In contrast, GDF3 expression in B16-F10 cells increased 7 days after tumor injection and maintained a high level until 14 days after injection.

the expression of GDF3 in mouse hepatoma G1 and G5 cell lines [29]. Unlike the mouse melanoma B16-F1 and B16-F10 cell lines, GDF3 expression was not observed in G1 or G5 cells in culture dish or in the cells during tumorigenesis (Figure 4A and data not shown).

To examine whether GDF3 promotes tumorigenesis of not only GDF3-expressing B16 melanomas but also tumors with no expression of GDF3, we transfected the mouse hepatoma G1 or G5 cell lines with empty or GDF3-expressing vectors, and injected the transfected cells into inbred BALB/c mice. Control transfected G1 or G5 cells formed tumors and the tumor size increased for 25 days (Figure 4B). Unlike B16 melanoma cells, forced expression of GDF3 did not result in acceleration of tumor growth in G1 or G5 cells (Figure 4B), indicating that the ability of GDF3 to promote tumorigenesis is specific to B16 melanoma that expresses GDF3 during s.c. progression.

Expression of genes encoding melanoma CSCs markers

We examined the mechanism by which GDF3 accelerates tumor growth. GDF3 inhibits bone morphogenetic

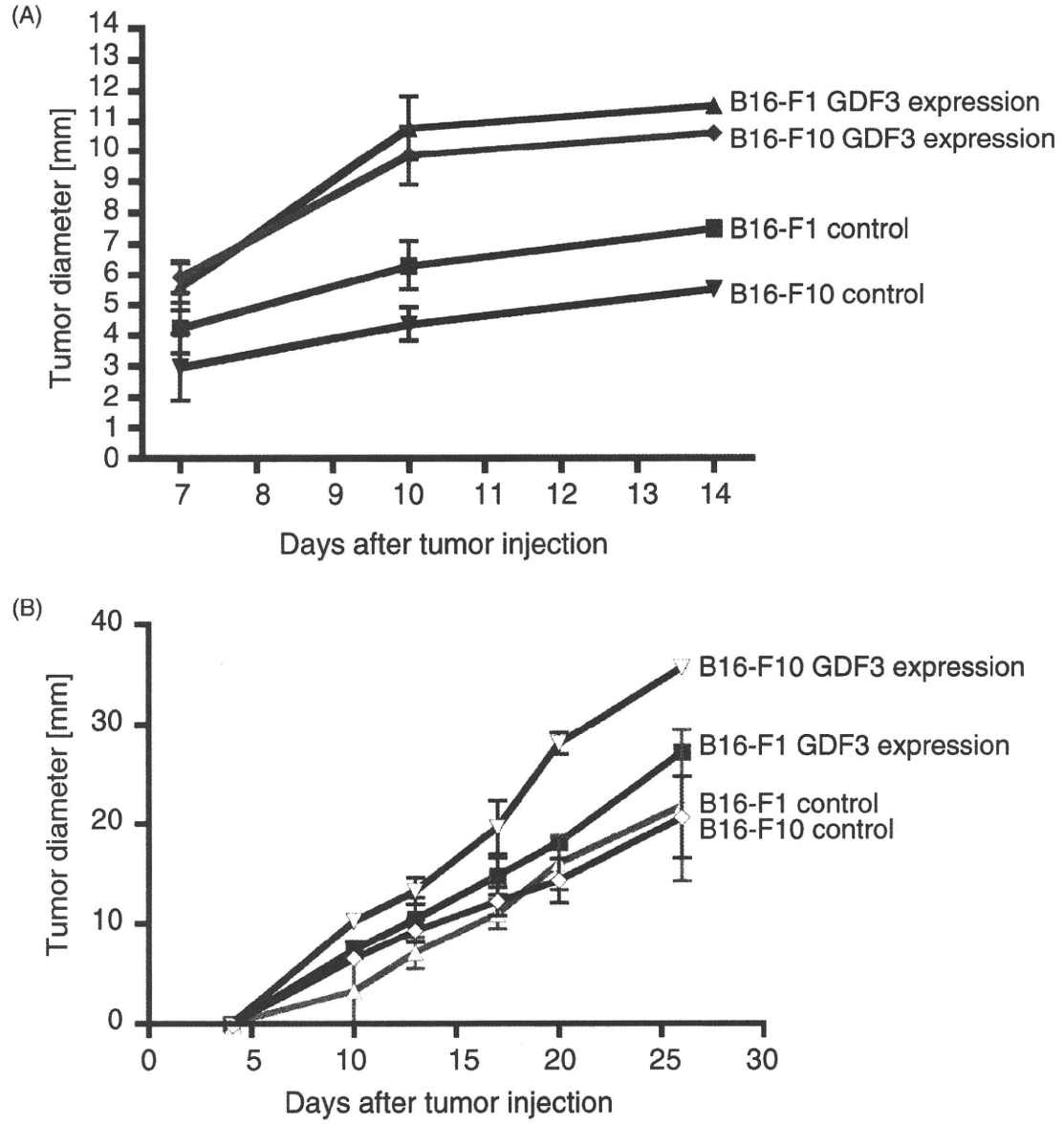

Figure 3 Effect of GDF3 expression on B16 melanoma tumorigenesis. B16-F1 and B16-F10 cells were transfected with empty or GDF3-expressing vectors. Twenty-four hours after transfection, 1×10^6 (A) or 1×10^5 (B) cells were injected subcutaneously into C57BL/6 mice and the tumor diameters were measured on the indicated day.

protein (BMP) signaling. Id1 is one of the transcription factors regulated by BMP signaling and its abnormal expression is observed in human cancers [27,30,31]. Therefore, we examined whether the GDF3 expression alters the Id1 expression; but no changes in Id1 expression was observed (Figure 5A).

ABCB5 is a marker of human melanoma CSCs, and CSCs with ABCB5 have a strong ability to generate tumors in xenotransplantation assays. Previously, Ning Gu and his colleagues showed that CD133-, CD44-, and CD24-positive B16-F10 cells show CSC-like feature and have strong ability to generate tumors [16]. We examined the expression of CD133, CD44, CD24, and ABCB5 during tumorigenesis of B16 melanoma cells transfected with empty or GDF3-expressing vectors. In B16-F1 cells, expression of ABCB5, CD44, and CD24 increased during tumorigenesis but CD133 expression was not observed at any time points (Figure 5B). Similar to B16-F1 cells,

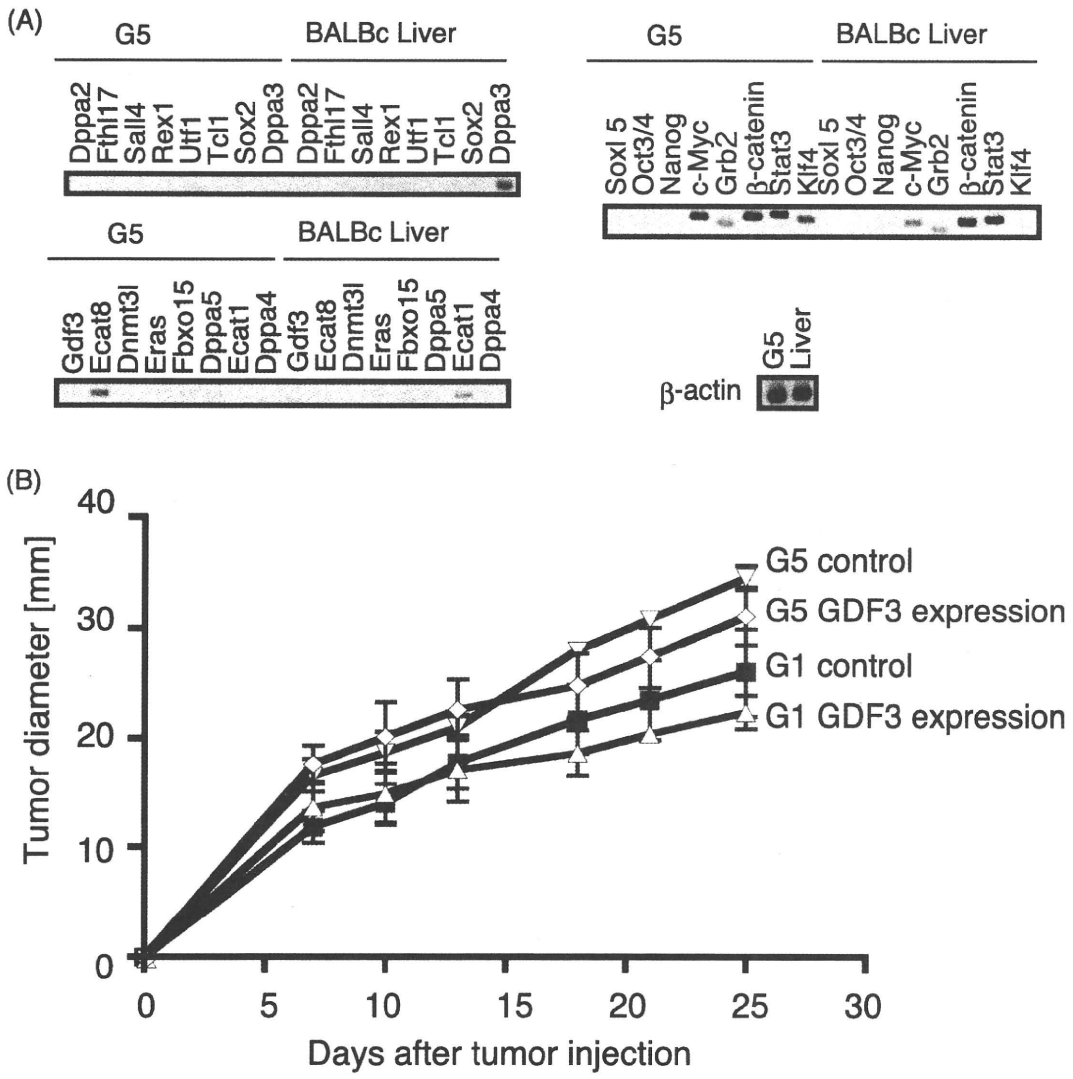

Figure 4 Effect of GDF3 expression on mouse hepatoma G1 or G5 cells. (A) Total RNA was extracted from G5 cells cultured in 10-cm dishes and BALB/c mouse liver, and RT-PCR analyses were carried out with primers listed in Table 1. (B) G1 and G5 cells were transfected with empty or GDF3-expressing vectors. Twenty-four hours after transfection, cells were injected subcutaneously into BALB/c mice and tumor diameters were measured on the indicated days. Two experiments with n = 4 were statistically analyzed.

CD24 and CD44 expression increased during B16-F10 tumorigenesis but ABCB5 expression was not observed (Figure 5C). In contrast, CD133 expression was observed during B16-F10 tumorigenesis (Figure 5C). Production of GDF3 did not affect CD133, ABCB5, and CD44 expression. However, CD24 expression was higher in GDF3-transfected B16-F1 and B16-F10 cells compared to that of empty vector-transfected B16-F1 and B16-F10 cells (Figure 5B and 5C). These data indicate that GDF3 expression leads to increased CD24 mRNA expression or an increase in the fraction of cells expressing CD24 mRNA.

Next, we performed FACS analysis to detect CD24- and CD44-positive cells. B16-F10 cells transfected with empty or GDF3-expressing vector were injected subcutaneously into C57BL/6 mice. Seven days after injection, the tumor was excised, and the tumor cells were stained with anti-CD24 and -CD44 antibodies. FACS analysis showed that tumor cells with GDF3-expressing vector contained more CD24 and CD44 double-positive cells than those transfected with the empty vector (Figure 5D and 5E). These data indicate that the expression of GDF3 increase the number of CD24 and CD44 double-positive cells during tumorigenesis.

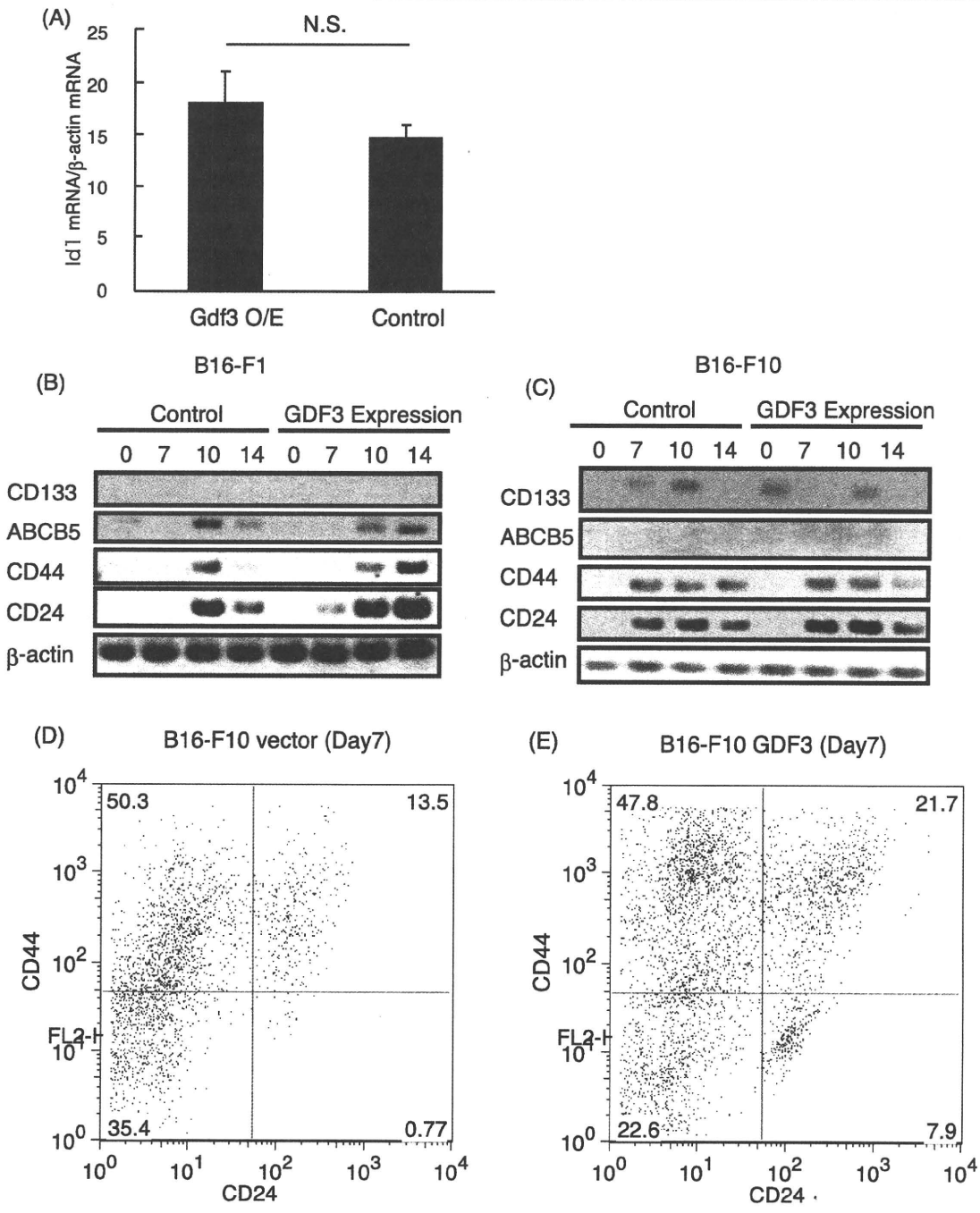

Figure 5 (A) B16-F1 cells transfected with an empty vector or a GDF3-expressing vector. Twenty-four hours after the transfection total RNA was extracted and RT-qPCR was performed to measure the Id1 expression. "N.S." stands for not statistically significant. (B, C) B16-F1 (B) or B16-F10 (C) cells were transfected with empty or GDF3-expressing vectors. Twenty-four hours after transfection cells were injected subcutaneously into C57BL/6 mice. Tumors were excised 7, 10, and 14 days after injection. Total RNA was extracted from tumors or cell from culture (day 0) and RT-PCR was performed. (D, E) B16-F10 cells were transfected with empty (D) or GDF3-expressing vectors (E) and 24 hours after the transfection cells were injected subcutaneously into C57BL/6 mice. The B16-F10 tumor was excised 7 days after injection. Cells were stained with a FITC-conjugated anti-CD24 antibody and a PE-conjugated anti-CD44 antibody. Cells were analyzed by FACS. One of three similar experiments is shown.

Expression levels of GDF3 in implant tumor cells

We finally confirmed that GDF3-transfected F1 and F10 cells continued to express GDF3 in implant tumors. RT-PCR analyses of excised tumors suggested that the transfected F1/F10 cells expressed the mRNA of GDF3 10 days after implantation although the levels of GDF3 mRNA decreased after 10 days compared to day 0 (Figure 6A). A negative control Soxl5 and a positive control β-actin were not affected by GDF3 transfection. Protein expression of GDF3 in F1 and F10 cells was examined by Western blotting using antibody against GDF3. A representative blotting profile is shown in Figure 6B. The protein as well as mRNA amounts of GDF3 were similar in F1 and F10 cells (Figure 6A,B). The results infer that the GDF3 message is translated into functional protein in these tumor cells and forced expression of GDF3 are still minimally expressed 10 days after transfection in these cells.

Discussion

We have shown that GDF3 mRNA increased during tumorigenesis in mouse melanoma B16-F1 and B16-F10 cells. Although the genotypic and phenotypic differences of these sublines of the same cell line origin was described earlier [32], genes responsible for their tumorigenic difference have not been fully elucidated. We found that GDF3 overexpression promotes tumorigenesis of mouse melanoma by B16-F1 and B16-F-10 cells but not hepatoma by G1 or G5 cells. Moreover, ectopic expression of GDF3 increased CD24 expression in both B16-F1 and B16-F10 cells. Human GDF3 is primarily expressed in embryonal carcinomas, testicular germ cell tumors, seminomas, and breast carcinomas. However, the role of GDF3 in tumorigenesis has not been shown yet. This is the first report that establishes a positive role of GDF3 in tumorigenesis.

Mouse melanoma CSC-like cells have a high degree of tumorigenicity and express CD133, CD44, and CD24 [16]. The expression of these three genes increased during B16-F10 tumorigenesis, and B16-F1 cells expressed CD44, CD24, and ABCB5 during tumorigenesis. We were unable to isolate the cells expressing CD44, CD24, and CD133 (or ABCB5) from B16 tumors injected into syngenic mice because of the low percentage of these cells in the overall population. However, the expression of CD24, CD44 and CD133 (or ABCB5) in melanoma B16 cells implies that CSC-like cells emerge during tumorigenesis. Indeed, we observed more CD24 and CD44 double-positive cells in GDF3-expressing B16-F10 cells than in control B16-F10 cells during tumorigenesis. But we have not yet shown the mechanism by which

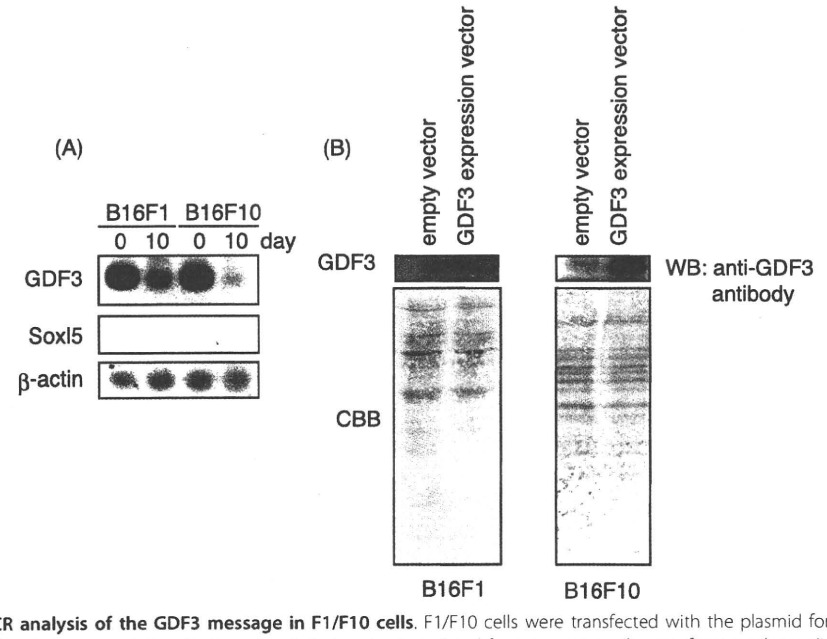

Figure 6 (A) RT-PCR analysis of the GDF3 message in F1/F10 cells. F1/F10 cells were transfected with the plasmid for expression of GDF3 (upper panel). Cells just before inoculation (indicated as 0 day) and cells isolated from tumors on day 10 after inoculation (indicated as day 10) were prepared and adjust the cell numbers. These cells were lysed and total RNA was extracted from the lysates. RT-PCR was performed to detect GDF3 as well as Soxl5 (nagative control, center panel) and β-actin (positive control, lower panel). PCR cycles are 32 rounds, 3 times less in those shown in Fig. 2C,D (B) Cell lysate (day 0) was subjected to SDS-PAGE (left 10% gel, right 8% gel) followed by immunoblotting. Lower panel- Commassie brilliant blue (CBB) staining of the blot. Upper panel- blots GDF3 band visualized by treating with anti-GDF3 mAb and then HRP-labeled 2nd Ab. No relevant band of GDF3 was detected by CBB staining.

GDF3 promotes turmorigenesis. The secondary effect of GDF3 expression on other genes should not be ruled out. One possible hypothesis is that GDF3 expression leads to an increase of some genes in CSC-like cells and these cells have a strong tumorigenic activity thus contributing to high GDF3 tumortigenicity.

Yamanaka and his colleagues firstly showed that the expression of four ES-specific genes, Klf4, Oct3/4, Sox2, and c-Myc, induces pluripotent stem cell proliferation from mouse embryonic and adult fibroblast cultures [10]. Another report also showed that another ES-specific gene Sall4 plays a positive role in the generation of pluripotent stem cells from blastocysts and fibroblasts [33]. In the current CSC theory, CSCs are derived from normal stem cells. Although several papers support this model, it is still unknown whether all CSCs are derived from normal stem cells [13]. In general, cancer cell genome becomes unstable because caretaker tumor suppressor genes are mutated during carcinogenesis [34]. Genome instability causes the expression of genes that are suppressed in normal tissues. In human ES cells, GDF3 supports the maintenance of the stem cell markers, Oct4, Nanog, and Sox2 [8,9]. Therefore, it is possible that some fraction of cancer cells may come to express these four genes *in vivo* leading to CSC formation from differentiated cancer cells, and GDF3 may promote this process. Another possibility of GDF3 role in tumorigensis is that GDF3 modulates TGF-mediated signaling, since it belongs to the TGF-β superfamily [8]. However, this model cannot explain why GDF3 expression increased only CD24 expression and not Id1 expression.

CD24 is a GPI-anchored sialoglycoprotein and is expressed in a variety of malignant cells [35]. CD24 participates in cell-cell contact and cell-matrix interaction and plays a role in cell proliferation. It is currently accepted that absence of CD24 on the tumor cell surface inhibits proliferative response and induces apoptosis in tumor cells, while up-regulation of CD24 promotes cell proliferation to increase tumor growth and metastasis [35,36]. Thus, the high CD24 level on tumor cells may predict poor prognosis in patients with cancer. In hepatocellular carcinoma CD24 level is actually correlated with patients' prognosis [36]. Our present finding furthers this notion and suggests that constitutive or forced expression of GDF3 in melanoma cells links the high CD24 expression accelerating tumor growth. By what mechanism TGF-β-like GDF3 induces up-regulation of CD24 on tumor cells, however, remains unknown.

In this regard, ectopic expression of GDF3 did not promote tumorigenesis of mouse hepatoma G1 and G5 cells. The expression profiles of CD24 in B16 melanoma sublines were parallel to those of GDF3, but hepatoma lines G1 and G5 had impaired the ability to induce GDF3-mediated CD24 expression. CD24 is rarely expressed on normal cells. Only limited subsets of myeloid cells are CD24-positive [36]. As the signal axis of this GDF3-derived CD24-inducing pathway is undetermined, it remains unsettled as to what is the molecular discrepancy between B16 F1/F10 melanoma cells and G-1/G5 hepatoma cells. Furthermore, the physiological role of the GDF3 signal and its downstream targets has not been elucidated. Yet the GDF3-CD24 pathway frequently turns positive when the cells are malignantly transformed [37] which may support the notion that CD24, when complexed with other molecules, alters its function for discrimination of danger signals [37].

Although possible experiments are in progress, another report suggests that CD24 is associated with Siglec-10 in humans or Siglec-G in mice serve as an innate immune receptor for endogenous self ligands named damage associated molecular pattern (DAMP) [38]. Accumulating evidence indicates that in tumor progression DAMP is released from damaged tissue or tumor cells and modulates both tumor and immune cells. Recent report suggested that the host inflammatory response to DAMP is partly controlled by a DAMP-CD24-Siglec axis [38]. We favor the speculation that the CD24 signals the presence of DAMP in a tumor micro environment, thereby augmenting inflammatory response to facilitate pathological tumor progression in GDF3-CD24 pathway-positive B16 F1/F10 but not -negative G-1/G-5 cells. Either way, this is the first report on the embryonic antigen GDF3 which is an inducer of CD24 and joins tumor cell proliferation. Further study may clarify the link between the CD24-Siglec G pathway and innate inflammatory response which occurs in invading tumor and facilitates to establish tumorigenesis.

Materials and methods

Cell lines and mice

B16-F1 and B16-F10 melanoma cells, G1 and G5 hepatoma cells were grown in RPMI1640 with 10% fetal bovine serum. These cell lines were transfectable, and transfection efficiencies were checked using the pEFBOS vector for expression of GFP. The transfection efficiencies were ~25% in F1 and F10 cells and ~20% in G-1 and G-5 cells (data not shown). We tried to establish stable clones constitutively expressing GDF3 in F1 and F10 cells, but failed to establish them. C57BL/6 and BALB/c mice (10-20 weeks of age) were purchased from Hokudo Co. (Sapporo, Japan). All mice were maintained under specific pathogen-free conditions in the animal facility of the Hokkaido University Graduate School of Medicine. Animal experiments were performed according to the guidelines set by the animal safety center, Japan.

RT-PCR

Total RNA from cells, tumors and normal tissues was isolated using the TRIZOL reagent (Invitrogen) according to the manufacturer's standard instructions. Reverse transcription was performed with random primers using the High Capacity cDNA reverse transcription kit (ABI). PCR was performed using primers listed in Table 1. These primer sets are applicable to the detection of the messages in mouse ES cells [10]. PCR cycles were usually 35 rounds, and otherwise described. We avoided quantitative interpretation of the results of RT-PCR analysis. The amplified DNA fragments were analyzed with 1% agarose gel and stained with etidium bromide.

Quantitative PCR

We used the following PCR primers: GDF3-F1, GDF3-R1, β-actin-F1, and β-actin R1 for quantitative PCR. Their sequences for GDF3 gene are listed in Table 1, and those of β-actin are a follows: β-actin-F1: TTT GCA GCT CCT TCG TTG C, and β-actin-R1: TCG TCA TCC ATG GCG AAC T. Quantitative PCR was performed by Step One real-time PCR system (ABI). The statistical comparisons were performed using the Student's *t* test between two groups.

Table 1 Primer sequences

Primer name	Primer sequence (F: forward)	Primer sequence (R: reverse)
Dppa2	agaagccgtgcaaagaaaaa	gttaaaatgcaacgggctgt
Fthl17	actttgggactgtgggactg	ttgatagcatcctcgcactg
Sall4	gcccctcaactgtctctctg	gggagctgttttctccactg
Rex1	caggttctggaagcgagttc	gacaagcatgtgcttcctca
Utf1	ttacgagcaccgacactctg	cgaaggaacctcgtagatgc
Tcl1	caccatgagggacaagacct	cttacaccgctctgcaatca
Sox2	atgggctctgtggtcaagtc	ccctcccaattcccttgtat
Dppa3	ctttgttgtcggtgctgaaa	tcccgttcaaactcatttcc
Gdf3	acctttccaagatggctcct	cctgaaccacagacagagca
Ecat8	tgtgtactggcaaccaaaa	ctgaggtcccatcagctctc
Dnmt3l	caagcctcgtgactttcctc	ccatggcattgatcctctct
Eras	atcctaacccccaactgtcc	caagcctcgtgactttcctc
Fbxol5	ctatgattggctgcgacaga	gtagtgtcgggaggcaatgt
Dppa5	cagtcgctggtgctgaaata	tccatttagcccgaatcttg
Ecatl	gaatgcctggaagatccaaa	aaatctcagctcgcctttca
Dppa4	agggctttcccagaacaaat	gcaggtatctgctcctctgg
Soxl5	cggcgtaagagcaaaaactc	tgggatcactctgagggaag
Oct3/4	ccaatcagcttgggctagag	ctgggaaaggtgtccctgta
Nanog	cacccacccatgctagtctt	accctcaaactcctggtcct
c-Myc	gcccagtgaggatatcttgga	atcgcagatgaagctctggt
Grb2	tcaatgggaaagatggcttc	gagcatttcttctgccttgg
β-catenin	gtgcaattcctgagctgaca	cttaaagatggccagcaagc
Stat3	agactacaggccctcagcaa	cctctgtcaggaaaggcttg
CD133	ctcatgcttgagagatcaggc	cgttgaggaagatgtgcacc
CD24	actctcacttgaaattgggc	gcacatgttaattactagtaaagg
CD44	gaaaggcatcttatggatgtgc	ctgtagtgaaacacaacacc
ABCB5	gtggctgaagaagccttgtc	tgaagccgtagccctcttta
GDF3	aaatgtttgtgttgcggtca	tctggcacaggtgtcttcag

Tumor transplantation

B16 melanoma cells or G1, G5 hepatoma cells were cultured in 10-cm dishes and harvested with 0.02% EDTA solution. Cells were washed two times with D-PBS. Mice were anesthetized with diethyl ether and tumor cells were injected subcutaneously into C57BL/6 or BALB/c mice. Tumor volumes were measured using a caliper every 1 or 2 days. Tumor volume was calculated using the formula: Tumor volume (cm^3) = (long diameter) × (short diameter) × (short diameter) × 0.4. Plotted data represent mean ± standard deviation (SD.).

Flow cytometry

Flow cytometry (FACS) was performed using FACS caliber. Excised B16-F1 and B16-F10 tumors were treated with collagenase D for 30 minutes and then suspended in RPMI 1640 medium. Cells were washed two times with FACS buffer (1 × PBS, 1% BSA, 2 mM EDTA). 1 × 10^6 cells were suspended in 50 μl of FACS buffer. Anti mouse CD22 and CD 44 mouse antibody (eBioscience) were added into the cell suspension, and the cells were incubated at 4°C for 45 minutes. After the incubation cells were washed twice with PBS, and analyzed by FACS caliber.

Western blot analysis

Cells were lysed in lysis buffer (20 mM Tris-HCl pH7.4, 150 mM NaCl, 1% NP-40, 10 mM EDTA, 25 mM iodoacetamide, 2 mM PMSF, protease inhibitor mixture (Roche)) and subjected to SDS-PAGE (8~10% gel) under reducing conditions followed by immunoblotting with anti-mouse GDF3 mAb or anti-β actin mAb (R&D Systems, Inc., Minneapolis, MN).

Acknowledgements

We thank Drs. T. Ebihara, H. Takaki. J. Kasamatsu, A. Watanabe, and H. Shime in our laboratory for their valuable discussions. Thanks are also due to Dr. Vijaya Lakshmi for her nice discussion and English review of the manuscript. This project was supported by Grants-in-Aid from the Ministry of Education, Science and Culture and the Ministry of Health, Labor, and Welfare of Japan, Mitsubishi Foundation, Mochida Foundation, NorthTec Foundation and Yakult Foundation.

Author details

[1]Department of Microbiology and Immunology, Graduate School of Medicine, Hokkaido University, Kita-15, Nishi-7, Kita-ku Sapporo 060-8638, Japan. [2]Department of Gastroenterology, Graduate School of Medicine, Hokkaido University, Kita-15, Nishi-7, Kita-ku Sapporo 060-8638, Japan.

Authors' contributions

HO, MM and TS designed the experiments. HO and NE carried out most of the experiments. TK and MA assigned this study to our laboratory. HO and TS wrote the manuscript. All authors read and approved the final manuscript.

Competing interests
The authors declare that they have no competing interests.

Received: 28 August 2010 Accepted: 15 October 2010
Published: 15 October 2010

References

1. Jones CM, Simon-Chazottes D, Guenet JL, Hogan BL: **Isolation of Vgr-2, a novel member of the transforming growth factor-beta-related gene family.** *Mol Endocrinol* 1992, **61**:1961-1968.
2. McPherron AC, Lee SJ: **GDF-3 and GDF-9: two new members of the transforming growth factor-beta superfamily containing a novel pattern of cysteines.** *J Biol Chem* 1993, **268**:3444-3449.
3. Caricasole AA, van Schaik RH, Zeinstra LM, Wierikx CD, van Gurp RJ, van den Pol M, Looijenga LH, Oosterhuis JW, Pera MF, Ward A, de Bruijn D, Kramer P, de Jong FH, van den Eijnden-van Raaij AJ: **Human growth-differentiation factor 3 (hGDF3): developmental regulation in human teratocarcinoma cell lines and expression in primary testicular germ cell tumours.** *Oncogene* 1998, **16**:95-103.
4. Ezeh UI, Turek PJ, Reijo RA, Clark AT: **Human embryonic stem cell genes OCT4, NANOG, STELLAR, and GDF3 are expressed in both seminoma and breast carcinoma.** *Cancer* 2005, **104**:2255-2265.
5. Skotheim RI, Autio R, Lind GE, Kraggerud SM, Andrews PW, Monni O, Kallioniemi O, Lothe RA: **Novel genomic aberrations in testicular germ cell tumors by array-CGH, and associated gene expression changes.** *Cell Oncol* 2006, **28**:315-326.
6. Gopalan A, Dhall D, Olgac S, Fine SW, Korkola JE, Houldsworth J, Chaganti RS, Bosl GJ, Reuter VE, Tickoo SK: **Testicular mixed germ cell tumors: a morphological and immunohistochemical study using stem cell markers, OCT3/4, SOX2 and GDF3, with emphasis on morphologically difficult-to-classify areas.** *Mod Pathol* 2009, **22**:1066-1074.
7. Clark AT, Rodriguez RT, Bodnar MS, Abeyta MJ, Cedars MI, Turek PJ, Firpo MT, Reijo Pera RA: **Human STELLAR, NANOG, and GDF3 genes are expressed in pluripotent cells and map to chromosome 12p13, a hotspot for teratocarcinoma.** *Stem Cells* 2004, **22**:169-179.
8. Levine AJ, Brivanlou AH: **GDF3 at the crossroads of TGF-beta signaling.** *Cell Cycle* 2006, **5**:1069-1073.
9. Levine AJ, Brivanlou AH: **GDF3, a BMP inhibitor, regulates cell fate in stem cells and early embryos.** *Development* 2006, **133**:209-216.
10. Takahashi K, Yamanaka S: **Induction of pluripotent stem cells from mouse embryonic and adult fibroblast cultures by defined factors.** *Cell* 2006, **126**:663-676.
11. Chen C, Ware SM, Sato A, Houston-Hawkins DE, Habas R, Matzuk MM, Shen MM, Brown CW: **The Vg1-related protein Gdf3 acts in a Nodal signaling pathway in the pre-gastrulation mouse embryo.** *Development* 2006, **133**:319-329.
12. Lapidot T, Sirard C, Vormoor J, Murdoch B, Hoang T, Caceres-Cortes J, Minden M, Paterson B, Caligiuri MA, Dick JE: **A cell initiating human acute myeloid leukaemia after transplantation into SCID mice.** *Nature* 1994, **367**:645-648.
13. Visvader JE, Lindeman GJ: **Cancer stem cells in solid tumours: accumulating evidence and unresolved questions.** *Nat Rev Cancer* 2008, **8**:755-768.
14. Schatton T, Murphy GF, Frank NY, Yamaura K, Waaga-Gasser AM, Gasser M, Zhan Q, Jordan S, Duncan LM, Weishaupt C, Fuhlbrigge RC, Kupper TS, Sayegh MH, Frank MH: **Identification of cells initiating human melanomas.** *Nature* 2008, **451**:345-349.
15. Quintana E, Shackleton M, Sabel MS, Fullen DR, Johnson TM, Morrison SJ: **Efficient tumour formation by single human melanoma cells.** *Nature* 2008, **456**:593-598.
16. Dou J, Pan M, Wen P, Li Y, Tang Q, Chu L, Zhao F, Jiang C, Hu W, Hu K, Gu N: **Isolation and identification of cancer stem-like cells from murine melanoma cell lines.** *Cell Mol Immunol* 2007, **4**:467-472.
17. Zhong Y, Guan K, Zhou C, Ma W, Wang D, Zhang Y, Zhang S: **Cancer stem cells sustaining the growth of mouse melanoma are not rare.** *Cancer Lett* 2010, **292**:17-23.
18. Cui W, Kong NR, Ma Y, Amin HM, Lai R, Chai L: **Differential expression of the novel oncogene, SALL4, in lymphoma, plasma cell myeloma, and acute lymphoblastic leukemia.** *Mod Pathol* 2006, **19**:1585-1592.
19. Ma Y, Cui W, Yang J, Qu J, Di C, Amin HM, Lai R, Ritz J, Krause DS, Chai L: **SALL4, a novel oncogene, is constitutively expressed in human acute myeloid leukemia (AML) and induces AML in transgenic mice.** *Blood* 2006, **108**:2726-2735.
20. Zhao W, Hisamuddin IM, Nandan MO, Babbin BA, Lamb NE, Yang VW: **Identification of Kruppel-like factor 4 as a potential tumor suppressor gene in colorectal cancer.** *Oncogene* 2004, **23**:395-402.
21. Wei D, Gong W, Kanai M, Schlunk C, Wang L, Yao JC, Wu TT, Huang S, Xie K: **Drastic down-regulation of Kruppel-like factor 4 expression is critical in human gastric cancer development and progression.** *Cancer Res* 2005, **65**:2746-2754.
22. Ohnishi S, Ohnami S, Laub F, Aoki K, Suzuki K, Kanai Y, Haga K, Asaka M, Ramirez F, Yoshida T: **Downregulation and growth inhibitory effect of epithelial-type Kruppel-like transcription factor KLF4, but not KLF5, in bladder cancer.** *Biochem Biophys Res Commun* 2003, **308**:251-256.
23. Dang DT, Chen X, Feng J, Torbenson M, Dang LH, Yang VW: **Overexpression of Kruppel-like factor 4 in the human colon cancer cell line RKO leads to reduced tumorigenecity.** *Oncogene* 2003, **22**:3424-3430.
24. Pandya AY, Talley LI, Frost AR, Fitzgerald TJ, Trivedi V, Chakravarthy M, Chhieng DC, Grizzle WE, Engler JA, Krontiras H, Bland KI, LoBuglio AF, Lobo-Ruppert SM, Ruppert JM: **Nuclear localization of KLF4 is associated with an aggressive phenotype in early-stage breast cancer.** *Clin Cancer Res* 2004, **10**:2709-2719.
25. Chen YJ, Wu CY, Chang CC, Ma CJ, Li MC, Chen CM: **Nuclear Kruppel-like factor 4 expression is associated with human skin squamous cell carcinoma progression and metastasis.** *Cancer Biol Ther* 2008, **7**:777-782.
26. Foster KW, Liu Z, Nail CD, Li X, Fitzgerald TJ, Bailey SK, Frost AR, Louro ID, Townes TM, Paterson AJ, Kudlow JE, Lobo-Ruppert SM, Ruppert JM: **Induction of KLF4 in basal keratinocytes blocks the proliferation-differentiation switch and initiates squamous epithelial dysplasia.** *Oncogene* 2005, **24**:1491-1500.
27. Ying QL, Nichols J, Chambers I, Smith A: **BMP induction of Id proteins suppresses differentiation and sustains embryonic stem cell self-renewal in collaboration with STAT3.** *Cell* 2003, **115**:281-292.
28. Giubellino A, Burke TR Jr: **Bottaro DP. Grb2 signaling in cell motility and cancer.** *Expert Opin Ther Targets* 2008, **12**:1021-1033.
29. Saeki Y, Seya T, Hazeki K, Ui M, Hazeki O, Akedo H: **Involvement of phosphoinositide 3-kinase in regulation of adhesive activity of highly metastatic hepatoma cells.** *J Biochem* 1998, **124**:1020-1025.
30. Kang Y, Chen CR, Massague J: **A self-enabling TGFbeta response coupled to stress signaling: Smad engages stress response factor ATF3 for Id1 repression in epithelial cells.** *Mol Cell* 2003, **11**:915-926.
31. Schindl M, Schoppmann SF, Strobel T, Heinzl H, Leisser C, Horvat R, Birner P: **Level of Id-1 protein expression correlates with poor differentiation, enhanced malignant potential, and more aggressive clinical behavior of epithelial ovarian tumors.** *Clin Cancer Res* 2003, **9**:779-785.
32. Ito A, Watabe K, Koma Y, Kitamura Y: **An attempt to isolate genes responsible for spontaneous and experimental metastasis in the mouse model.** *Histol Histopathol* 2002, **17**:951-959.
33. Tsubooka N, Ichisaka T, Okita K, Takahashi K, Nakagawa M, Yamanaka S: **Roles of Sall4 in the generation of pluripotent stem cells from blastocysts and fibroblasts.** *Genes Cells* 2009, **14**:683-694.
34. Levitt NC, Hickson ID: **Caretaker tumour suppressor genes that defend genome integrity.** *Trends Mol Med* 2002, **8**:179-186.
35. Kristiansen G, Winzer KJ, Mayordomo E, Bellach J, Schluns K, Denkert C, Dahl E, Pilarsky C, Altevogt P, Guski H, Dietel M: **CD24 expression is a new prognostic marker in breast cancer.** *Clin Cancer Res* 2003, **9**:4906-4913.
36. Yang XR, Xu Y, Yu B, Zhou J, Li JC, Qiu SJ, Shi YH, Wang XY, Dai Z, Shi GM, Wu B, Wu LM, Yang GH, Zhang BH, Qin WX, Fan J: **CD24 is a novel predictor for poor prognosis of hepatocellular carcinoma after surgery.** *Clin Cancer Res* 2009, **15**:5518-5527.
37. Liu Y, Chen GY, Zheng P: **CD24-Siglec G/10 discriminates danger- from pathogen-associated molecular patterns.** *Trends Immunol* 2009, **30**:557-561.
38. Chen GY, Tang J, Zheng P, Liu Y: **CD24 and Siglec-10 selectively repress tissue damage-induced immune responses.** *Science* 2009, **323**:1722-1725.

doi:10.1186/1756-9966-29-135
Cite this article as: Ehira *et al.*: An embryo-specific expressing TGF-β family protein, growth-differentiation factor 3 (GDF3), augments progression of B16 melanoma. *Journal of Experimental & Clinical Cancer Research* 2010 **29**:135.

Frontline

European Journal of Immunology

DEAD/H BOX 3 (DDX3) helicase binds the RIG-I adaptor IPS-1 to up-regulate IFN-β-inducing potential

Hiroyuki Oshiumi, Keisuke Sakai, Misako Matsumoto and Tsukasa Seya

Department of Microbiology and Immunology, Hokkaido University Graduate School of Medicine, Kita-ku, Sapporo, Japan

Retinoic acid-inducible gene-I (RIG-I)-like receptors (RLR) are members of the DEAD box helicases, and recognize viral RNA in the cytoplasm, leading to IFN-β induction through the adaptor IFN-β promoter stimulator-1 (IPS-1) (also known as Cardif, mitochondrial antiviral signaling protein or virus-induced signaling adaptor). Since uninfected cells usually harbor a trace of RIG-I, other RNA-binding proteins may participate in assembling viral RNA into the IPS-1 pathway during the initial response to infection. We searched for proteins coupling with human IPS-1 by yeast two-hybrid and identified another DEAD (Asp-Glu-Ala-Asp) box helicase, DDX3 (DEAD/H BOX 3). DDX3 can bind viral RNA to join it in the IPS-1 complex. Unlike RIG-I, DDX3 was constitutively expressed in cells, and some fraction of DDX3 is colocalized with IPS-1 around mitochondria. The 622-662 a.a DDX3 C-terminal region (DDX3-C) directly bound to the IPS-1 CARD-like domain, and the whole DDX3 protein also associated with RLR. By reporter assay, DDX3 helped IPS-1 up-regulate IFN-β promoter activation and knockdown of DDX3 by siRNA resulted in reduced IFN-β induction. This activity was conserved on the DDX3-C fragment. DDX3 only marginally enhanced IFN-β promoter activation induced by transfected TANK-binding kinase 1 (TBK1) or I-kappa-B kinase-ε (IKKε). Forced expression of DDX3 augmented virus-mediated IFN-β induction and host cell protection against virus infection. Hence, DDX3 is an antiviral IPS-1 enhancer.

Key words: DDX3 · IFN-β · IPS-1 · RIG-I-like receptors · Viral infection

See accompanying Commentary by Mulhern and Bowie

Introduction

Retinoic acid-inducible gene-I (RIG-I) and melanoma differentiation-associated gene 5 (MDA5) are cytoplasmic RNA helicases [1–3], which signal the presence of viral RNA through the adaptor, IFN-β promoter stimulator-1 (IPS-1) (also known as mitochondrial antiviral signaling protein/caspase recruitment domain (CARD) adaptor inducing IFN-β (Cardif)/virus-induced signaling adaptor) to produce IFN-β [4–7]. IPS-1 localizes on the outer membrane of the mitochondria *via* its C-terminus [6]. Its N-terminus consists of a CARD domain, which interacts with the CARD domains of RIG-I and MDA5. Viral RNA resulting from penetration or replication are believed to assemble in the CARD-interacting helicase complex to activate the cytoplasmic IFN-inducing pathway. Although non-infected cells usually express minimal amounts of RIG-I/MDA5, the final output of type I IFN is efficiently induced at an early stage of infection to protect host cells from viral spreading.

Once IPS-1 is activated, the kinase complex consisting of TANK-homologous proteins and virus-activated kinases induce nuclear translocation of IFN regulatory factor-3 (IRF-3) to activate the IFN promoter [8]. NAK-associated protein 1, TANK-binding kinase 1 (TBK1) and I-kappa-B kinase-ε (IKKε) are components of the kinase complex that phosphorylates IRF-3 to induce type I IFN [9, 10]. RIG-I recognizes products of various RNA viruses, while MDA5 recognizes products of picornaviruses

Correspondence: Dr. Tsukasa Seya
e-mail: seya-tu@pop.med.hokudai.ac.jp

[1, 11]. RIG-I and MDA5 share the helicase domain, which is classified into the DEAD (Asp-Glu-Ala-Asp) box helicase family, and the domain can bind to various RNA structures. 5′-triphosphate RNA or short dsRNA is a ligand of RIG-I, whereas long dsRNA is a ligand of MDA5 [1, 12]. However, these RIG-I-like receptors (RLR) are usually up-regulated to a sufficient level secondary to IFN stimulation, suggesting that other molecular mechanisms are responsible for the initial sensing of viral RNA.

Here, we looked for molecules that bind IPS-1 by yeast two-hybrid, and found a DEAD box helicase, DDX3 (DEAD/H BOX 3), as a component of the complex of IPS-1. DDX3 facilitated IPS-1-mediated IFN-β induction to confer high antiviral potential on early infection phase of host cells. This is the first report showing that DDX3 is an IPS-1 complement factor for antiviral IFN-β induction in host infectious cells.

Results

Involvement of DDX3 in the IPS-1 complex

IPS-1 is constitutively present on the mitochondrial membrane and plays a central role in the cytoplasmic IFN-inducing pathway. We searched for proteins that bind IPS-1 in yeast. Using bait plasmids with the IPS-1 CARD region (aa 6–136), we screened a human lung cDNA library to isolate IPS-1 CARD-interacting proteins. We identified one clone, #62 that encodes the DDX3 C-terminal region (aa 276–662), which included partial DEAD box and helicase superfamily C-terminal regions (Fig. 1A). Their interaction was confirmed in HEK293FT cells by immunoprecipitation (IP), where DDX3 and IPS-1 were coupled (Fig. 1B). We confirmed that the C-terminal fragments of DDX3, at least 622-662 a.a, bound IPS-1 (data not shown). Taken together with the results of the yeast two-hybrid assay, the C-terminal portions of DDX3 directly bind the CARD-like region of IPS-1.

RIG-I and MDA5 helicases also bind the IPS-1 CARD domain [4]. In general, RNA helicases make a large molecular complex, and sometimes form homo- or hetero-oligomers. RIG-I binds to LGP2 helicase, and forms homo-oligomers during Sendai virus infection [11]. Hence, we examined whether DDX3 was associated with the RLR proteins by i.p. RIG-I and MDA5 co-precipitated with DDX3 (Fig. 2A), suggesting that DDX3 is involved in the complex of IPS-1 that interacts with RIG-I and/or MDA5. DDX3 bound the C-terminal helicase domain including the RD region of RIG-I (Fig. 2B). Thus, additional interaction may occur between DDX3 and RIG-I/MDA5. IPS-1 localizes to the membrane of mitochondria [6]. Three-color imaging analysis indicated that DDX3 in part co-localized to the IPS-1-mitochodria complex in non-stimulated resting HeLa cells, which express undetectable amounts of RLR (Fig. 2C and data not shown). These results together with accumulating evidence infer that non-infected cells harbor the complex of DDX3 and IPS-1 with minimal amounts of RIG-I/MDA5.

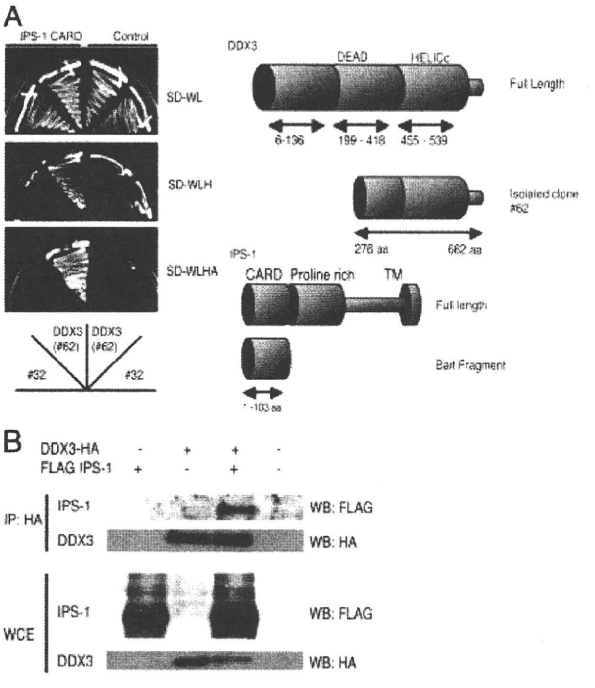

Figure 1. DDX3 binds IPS-1. (A) DDX3 partial cDNA fragment (aa 276–662) isolated by the yeast two-hybrid screening interacted with the IPS-1 CARD region (aa 1–103) in yeast. Tryptophan- and leucine-depleted synthetic dextrose medium plate (SD-WL) is non-selective, and tryptophan-, leucine- and histidine-depleted synthetic dextrose medium plate (SD-WLH) and tryptophan-, leucine-, histidine- and alanine-depleted synthetic dextrose medium (SD-WLHA) plates are selective plates. Empty bait plasmid (pGBKT7) was used for a negative control. (B) FLAG-tagged IPS-1 and HA-tagged DDX3 expression vectors were transiently transfected into HEK293FT cells by FuGeneHD reagent. 24 h after transfection, cell lysates were prepared, and IP was carried out using anti-HA Ab. The immunoprecipitates were analyzed by western blot using anti-HA or FLAG Ab. Data are representative of three independent experiments.

DDX3 promotes IPS-1-mediated IFN-β promoter activation

Forced expression of IPS-1 causes the activation of transcription from the IFN-β promoter. To ascertain the role of DDX3 in IFN-β production, we carried out reporter gene analysis to see the enhancing effect of DDX3 on IPS-1-mediated IFN-β promoter activation. Overexpression of DDX3 alone caused little activation of the promoter; however, the promoter activation was more augmented by minimal addition of DDX3 to IPS-1 than by overexpressed IPS-1 alone (Fig. 3A). This suggested that DDX3 enhanced IPS-1-mediated signaling despite the lack of RIG-I overexpression. To establish which region of DDX3 is important for IFN-β enhancer activity, partial DDX3 fragments were overexpressed with IPS-1, and IFN-β promoter activation was examined. The N-terminal region (aa 1–224, aa 224–487, aa 488–621) barely enhanced promoter activation (data not shown), but the C-terminal region (622–662) activated the promoter (Fig. 3B). These data indicated that the C-terminal region of DDX3 is important for the binding to IPS-1 and potentiation of the IPS-1 pathway.

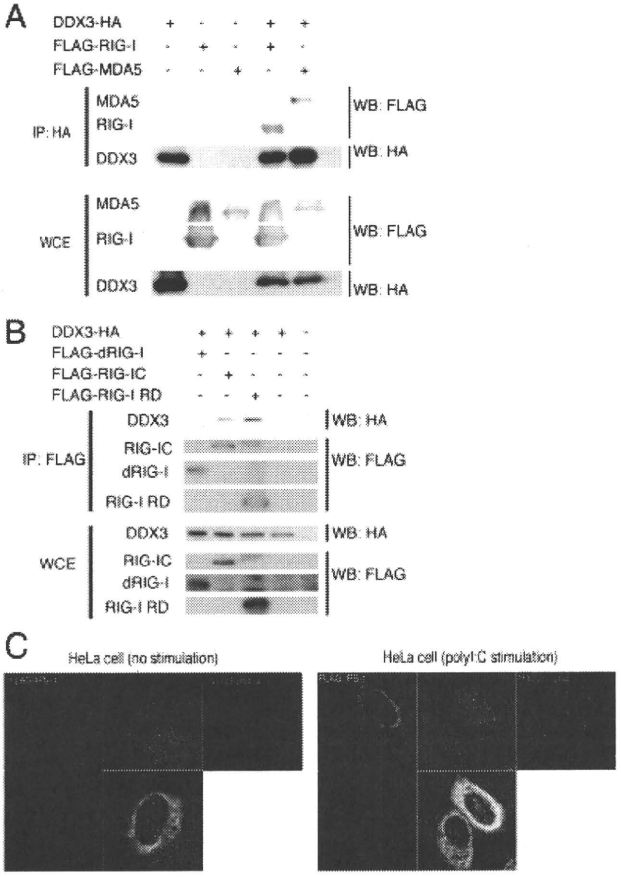

Figure 2. DDX3 joins the complex of RIG-I, MDA5 and IPS-1. (A) RIG-I and MDA5 co-precipitate with DDX3. HA-tagged DDX3 was expressed in HEK293FT cells, together with FLAG-tagged MDA5 or RIG-I, and 24 h after transfection, IP was performed using anti-HA Ab and analyzed by western blotting. (B) The C-terminal region of RIG-I participates in complex formation with DDX3. FLAG-tagged RIG-I fragments and HA-tagged DDX3 were expressed in HEK293 cells, and 24 h after transfection, IP was performed using anti-HA Ab and analyzed by western blotting. (C) DDX3 colocalizes with IPS-1. Flag-tagged IPS-1 and HA-tagged DDX3 were transfected into HeLa cells together with or without polyI:C. After 24 h, cells were fixed with formaldehyde and stained with anti-HA polyclonal and anti-FLAG monoclonal Ab. Alexa488 (DDX3-HA) or Alexa633 Ab was used for second Ab. Mitochondria was stained with Mitotracker Red. DDX-3 partially colocalized with IPS-1. Data are representative of three independent experiments.

DDX3 as a component of initial RNA sensor

RIG-I and MDA5 are IFN-inducible proteins, only traces of which exist in an early phase (< 2 h) in the cytoplasm where viral RNA replicate. Previous reports showed that DDX3 binds RNA of poly rA or duplexed RNA [13, 14], and our protein analysis solidified this issue: DDX3 efficiently bound polyI:C and stem-loop RNA of viral origin in a solution (data not shown). DDX3 as well as IPS-1 were expressed even without any stimulation (Fig. 2C and 4A and B) and bound each other in the cytoplasm (Fig. 2C). Hence, DDX3 is a cytoplasmic molecule that can detect viral RNA produced in infected cells.

Knockdown studies suggested that polyI:C-mediated IFN promoter activation was abrogated in DDX3-deficient cells even in the presence of overexpressed RIG-I or MDA5 (Fig. 5). DDX3 silencing happened with two different siRNA. Thus, DDX3 may enable RIG-I and IPS-1 to confer activation of the cytoplasmic RNA-sensing pathway on virus-infected cells.

The IFN-β-inducing pathway involves IRF-3 kinases TBK1 and IKKε, which may be targets of DDX3 [15, 16]. By *in vitro* reporter analysis, increasing amounts of DDX3 barely affected IFN-β promoter activation by TBK1 and IKKε (Fig. 6A and B). Slight TBK1-enhancing activity could manage to be detected with DDX3 when decreasing amounts of TBK1 was used in the assay (Fig. 6C and D).

HeLa cells induced the mRNA of RIG-I and IFN-β in response to polyI:C stimulation within 1 h (Fig. 4A). More exactly, IFN-β induction was ~30 min faster than RIG-I induction in response to polyI:C. IFN-β mRNA induction was peaked around 3 h post stimulation, while RIG-I induction continued to increase > 3 h (Fig. 4A). When HEK293 cells were infected with vesicular stomatitis virus (VSV) (a RIG-I-stimulating virus), the IFN-β mRNA was induced from 6 h, and by that time no RIG-I message was generated (Fig. 4B–D). The RIG-I message began to appear > 8 h and was markedly increased (Fig. 4B and D). In either case, no up-regulation was observed with DDX3 but sufficiently present in the cytoplasm (Fig. 4C). Furthermore, overexpression of DDX3 in HeLa cells resulted in potential prevention of VSV propagation (Fig. 7). However, the distribution profiles of DDX3 and IPS-1 were barely altered in response to polyI:C stimulation (Fig. 2C). The results allow us to interpret that when viral RNA enter the cytoplasm of infected cells, the RNA first induce a small amount of IFN-β in conjunction with the complex containing trace RIG-I and then the induced IFN-β fosters intensive RIG-I/MDA5 induction. The complex is reconstituted together with upcoming RIG-I/MDA5 to amplify the cytoplasmic IFN-inducing pathway. Although the molecular reconstitution was not visible with overexpressed proteins by confocal analysis, DDX3 may act as an enhancing factor for initial RNA-sensing by the IPS-1 complex and conducts the rapid response to viral RNA to facilitate the IPS-1 signaling.

Discussion

We identified DDX3 as a protein that bound to the IPS-1 CARD region, duplexed RNA and RLR. Although the DDX3 helicase domain is a DEAD box type similar to those of RIG-I and MDA5, DDX3 does not have a signaling domain corresponding to the CARD domain. Therefore, DDX3 may not act as a signal sensor of RNA viruses, as RIG-I and MDA5 do. Considering the role of DDX3 in host RNA metabolism, it is more likely that DDX3 acts as a scaffold for RIG-I (even under the presence of low copy numbers of RIG-I) and intensifies IPS-1 signaling similar to LGP2 [11, 17]. RNA molecules usually form a complex with various

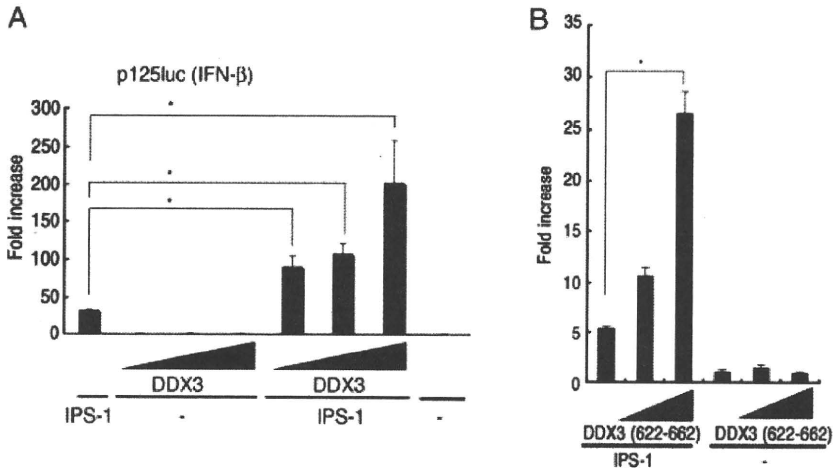

Figure 3. The C-terminal region of DDX3 participates in enhancing IPS-1-mediated IFN-β promoter activation. (A) Activation of IFN-β promoter was examined by reporter gene assay. HEK293 cells were transfected with DDX3- (100, 200 or 300 ng) and/or IPS-1 (100 ng)-encoding plasmids, together with reporter (p125luc) and control plasmids (Renilla luciferase) into 24-well plates. (B) The plasmids for expression of DDX3 (622-662 aa) and IPS-1 or the former only were transfected into HEK293 cells in 24-well plates together with p125luc reporter plasmid. After 24 h, the activation of reporter was measured. Data show mean fold induction+SD of three independent assays. $^{*}p<0.05$, Student's t-test.

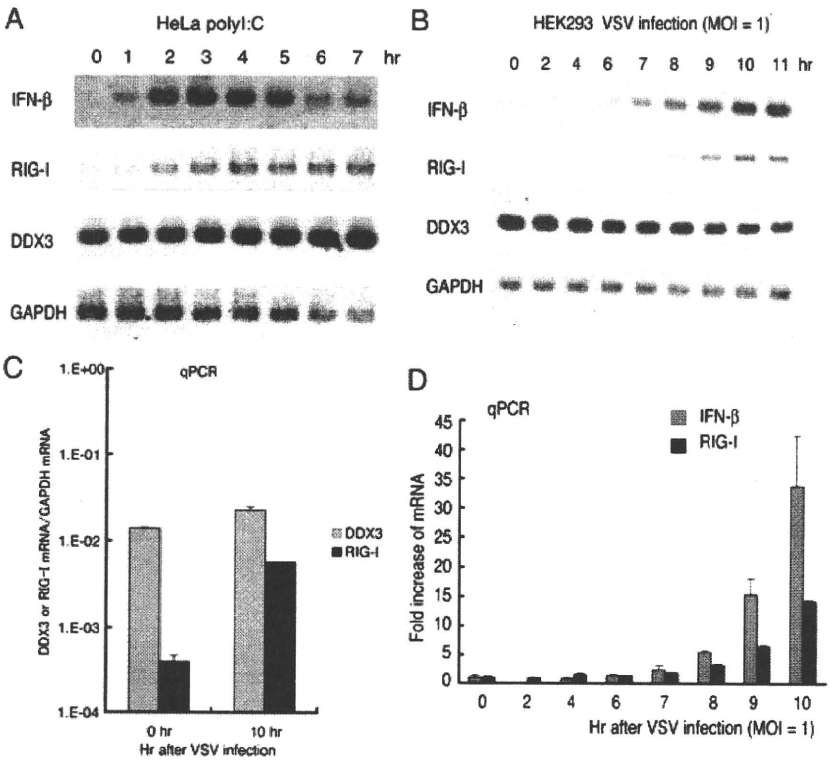

Figure 4. Earlier induction of IFN- than RIG-I in virus-infected cells. (A) Early induction of IFN-β in response to polyI:C. HeLa cells were stimulated with 50 μg/mL of polyI:C for indicated hours. Total RNA was extracted with TRIZOL and RT-PCR was carried out to examine the kinetics of expressions of DDX3, IFN-β, RIG-I and GAPDH (control). (B) IFN-β mRNA induction by VSV infection. HEK293 cell were infected with VSV at MOI = 1, and then total RNA was extracted with TRIZOL reagents at indicated times. The reverse transcription with random primers and PCR at 33 cycle were performed to detect RIG-I, DDX3 or IFN-β expression. Data are representative of three independent experiments. (C) Marked induction of RIG-I in VSV-infected cells. HEK293 cells were infected with VSV at MOI = 1, and then the total RNA was extracted with TRIZOL reagent at indicated times. The relative amounts of RIG-I or DDX3 mRNA were quantified by RT-qPCR, in which the mRNA of GAPDH was used for endogenous internal control. (D) Fold increase of IFN-β or RIG-I mRNA by VSV infection. The amount of IFN-β or RIG-I cDNA was determined by quantitative PCR. The fold increases were calculated by dividing the values of each time point by that of 0 h sample of IFN-β or RIG-I. Data show mean+SD pooled from three independent experiments.

proteins, such as 5′-end capping enzymes or translation initiation factors. Viral RNA also tends to couple with host proteins to replicate and translate RNA. DDX3 capturing RNA may function either in the molecular complex of RIG-I/MDA5/IPS-1 or in the complex of the translation machinery.

Recently, DDX3 was reported to up-regulate IFN-β induction by interacting with IKKε in the kinase complex [18]. IKKε is an NF-κB-inducible gene, whereas the DDX3-IPS-1 complex is constitutively present prior to infection. DDX3 may bind IKKε after IKKε is generated secondary to NF-κB activation [15]. Another report suggested that DDX3 interacts with TBK1 to synergistically stimulate the IFN-β promoter [16]. The report further suggested that DDX3 is recruited to the IFN promoter and acts like a transcription factor [16]. These reports also show that not C-terminal but N-terminal region of DDX3 is required for enhancing the IKKε- or TBK1-mediated IFN promoter activation. We showed that unlike these previous reports, the C-terminal region of DDX3 is important for the IPS-1 activation. These observations indicate that DDX3 is involved in RIG-I signaling at multiple steps. The involvement of DDX3 at several steps is not surprising, because DDX3 plays several roles in RNA metabolisms, such as RNA translocation or mRNA translation.

In cytoplasm, there are large amounts of DDX3 and only trace amounts of RIG-I in resting cells. Therefore, when the virus initially infects human cells, the viral RNA would encounter DDX3 before RIG-I capture the viral RNA. We demonstrated that the initial IPS-1 complex for RNA-sensing involves DDX3 in addition to trace RIG-I to cope with the early phase of infection. This IPS-1 complex activates downstream signal by involving a minute amount of viral RNA. What happens in actual viral infection is to first induce IFN-β and then RIG-I (Fig. 4B), suggesting that the initial IFN-β mRNA arises independent of the virus-induced RIG-I. Once IFN-β and RIG-I mRNA are up-regulated by viral RNA, the IPS-1 complex turns constitutionally different: the complex contains high amounts of RIG-I, which may directly capture viral RNA without DDX3. Our results indicate that the early IPS-1 complex formed in the early stages of virus-infected cells induce minute IFN-β with a mode different from the conventional IPS-1 pathway that RIG-I solely capture viral RNA and activates IPS-1. By retracting DDX3 from the complex by siRNA, only a minimal IFN-β response emerges merely with preexisting RIG-I and IPS-1, suggesting DDX3 to be a critical signal enhancer in the early IPS-1 complex. Development of a method to chase endogenous DDX3 will be required to test our interpretation.

The RIG-I generation occurring > 8 h post RNA virus challenge makes the complex direct the conventional IFN-inducing pathway harboring sufficient RIG-I/MDA5. Previous reports [13, 14] and our RNA-binding analysis also speculated that one of the RNA-capture proteins is DDX3 since DDX3 tightly binds polyI:C and dsRNA in fluid phase. These RNA-capture proteins may have a role in the IPS-1-involving molecular platform in cells with early virus infection when only a trace RIG-I protein is expressed. This interpretation fits the result that DDX3 acts predominantly on an early phase of virus infection (Fig. 4B and 7).

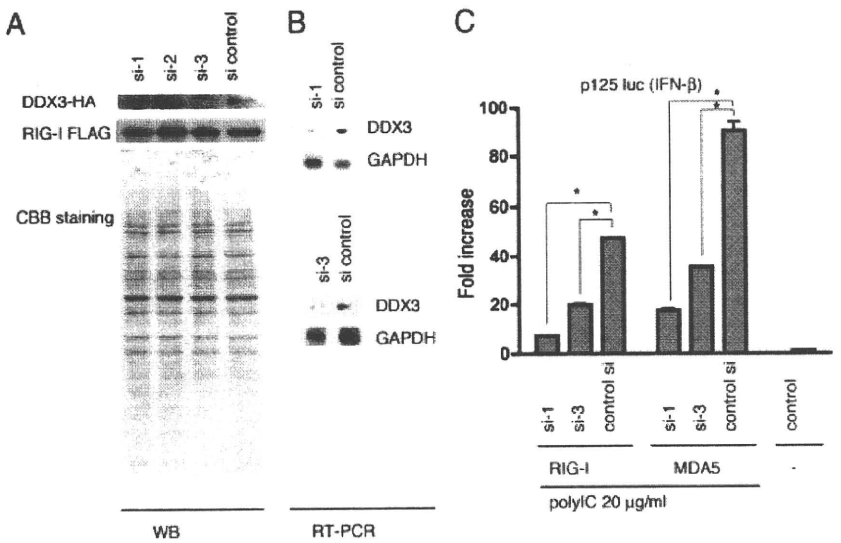

Figure 5. Knockdown of DDX3. (A) Negative control or DDX3 targeting siRNA (20 pmol), DDX3 si-1, -2 or -3, were transfected into HEK293 cells in 24-well plates, together with HA-tagged DDX3 or FLAG-tagged RIG-I expression plasmids, and after 48 h, cell lysates were prepared and analyzed by western blotting with anti-HA or anti-FLAG Ab, and the same membrane was stained with CBB. (B) DDX3 si-1, -3 or control siRNA was transfected into HEK293 cells, and after 48 h, expression of endogenous DDX3 mRNA was examined by RT-PCR. (C) DDX3 si-1, -3 or control siRNA was transfected into HEK293 cells with reporter plasmids and RIG-I- or MDA5 expression plasmid (100 ng). Forty-eight hours after transfection, cells were stimulated with polyI:C (20 μg/mL) with dextran for 4 h, and activation of the reporter was measured. siRNA for DDX3 reduced RIG-I- or MDA5-mediated p125luc activation. Data are representative of three independent experiments (A,B). Data show mean fold increase+SD pooled from three independent experiments (C). *$p<0.05$, Student's t-test.

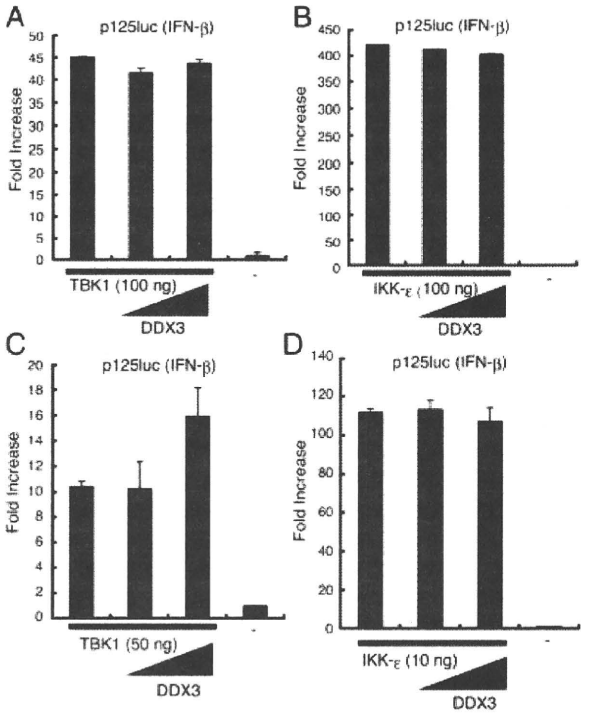

Figure 6. TBK1 and IKKε are not main targets for DDX3-mediated IFN-β up-regulation. (A–D) The activation of IFN-β promoter was examined by reporter gene assay. HEK293 cells were transfected in 24-well plates with DDX3 (0, 100 or 300 ng)-, TBK1 (0, 50 or 100 ng)- or IKKε (0, 10 or 100 ng)-encoding plasmid together with reporter (p125luc) and control plasmid. After 24 h, the cell lysate was prepared and the luciferase activities were measured. Data show mean+SD of three independent experiments.

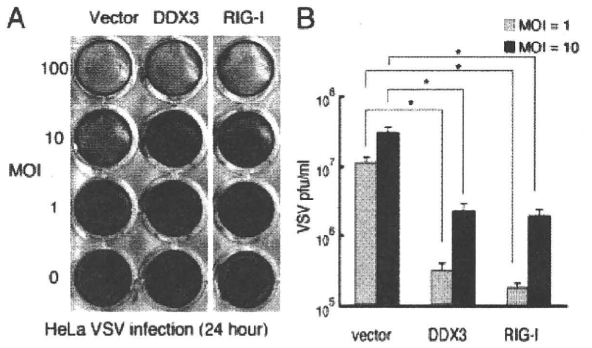

Figure 7. VSV infection is suppressed by overexpressed DDX3. (A) HeLa cells were transfected with DDX3, RIG-I or empty vector. After 24 h, the transfected cells were infected with VSV at indicated MOI. 24 h after VSV infection, the cells were fixed with formaldehyde and stained with crystal violet. (B) The VSV titers of culture supernatant of HeLa cells infected with VSV at MOI = 1 or 10 were measured by plaque assay. Data show mean+SD of three independent experiments. *$p<0.05$, Student's *t*-test.

Proteins involved in type I IFN induction are found ubiquitinated for their functional regulation. It has been reported that TRIM25 [19] and Riplet/RNF135 [20] act as ubiquitin ligases to activate RIG-I for IFN-β induction in their different sites of RIG-I ubiquitination. Another ubiquitin ligase RNF125 polyubiquitinates RIG-I through Lys48, leading to degradation of RIG-I [21]. The RIG-I level is highly susceptible to not only IFN but also ubiquitination in host cells. In addition, many viral factors may suppress the RIG-I function. It remains unknown what factor maintains a minimal level of RIG-I/MDA5 in resting cells. We favor the interpretation that DDX3 can be an alternative factor for compensating the low RLR contents in a certain infectious situation such that RIG-I is degraded or poorly up-regulated by other viral factors.

DDX3 is functionally complicated since its protective role against viruses may be modulated after the synthesis of viral proteins. DDX3 couples with the HCV core protein in HCV-infected cells and promotes viral replication [22]. This alternative function of DDX3 is accelerated by the HCV core protein, since the core protein withdraws DDX3 from the IFN-β-inducing facility, leading to suppression of IFN-β induction and positive regulation of HCV propagation in infected cells. DDX3 is also involved in HIV RNA translocation [14]. The DDX3 gene is conserved among eukaryotes, and Ded1 is a budding yeast homolog [23]. Ded1 helicase is essential for initiation of host mRNA translation, and human DDX3 can complement the lethality of Ded1-null yeast cells [24, 25]. Hence, another function of DDX3 is to bind viral RNA to modulate RNA replication and translocation. It is not surprising that DDX3 is implicated in various steps of RNA metabolism in cells with both host and viral RNA.

Materials and methods

Cell culture and reagents

HEK293 cells and HEK293FT cells were maintained in Dulbecco's Modified Eagle's low or high glucose medium (Invitrogen, Carlsbad, CA, USA) supplemented with 10% heat-inactivated FBS (Invitrogen) and antibiotics. HeLa cells were maintained in MEM (Nissui, Tokyo, Japan) supplemented with 10% heat-inactivated FBS. Anti-FLAG M2 mAb, anti-HA polyclonal Ab, were purchased from Sigma-Aldrich (St. Louis, MO, USA). Alexa Fluor®-conjugated secondary Ab were from Invitrogen.

Plasmids

DDX3 cDNA encoding the entire ORF was cloned into pCR-blunt vector using primers, DDX3N F-Xh (CTC GAG CCA CCA TGA GTC ATG TGG CAG TGG AA) and DDX3C R-Ba (GGA TCC GTT ACC CCA CCA GTC AAC CCC) from human lung cDNA library. To make an expression plasmid, HA tag was fused at the C-terminal end of the full length DDX3 (pEF-BOS DDX3-HA). pEF-BOS DDX3 (1–224 aa) vector was made by using primers DDX3 N-F-Xh and DDX3D1 (GGA TCC GGC ACA AGC CAT CAA GTC TCT TTT C).

pEF-BOS DDX3-HA (225–662) was made by using primers DDX3D2-3 (CTC GAG CCA CCA TGC AAA CAG GGT CTG GAA AAA C) and DDX3C R-Ba. To make pEF-BOS DDX3-HA (225–484) and pEF-BOS DDX3-HA (485–663), the primers DDX3D2 R-Ba (GGA TCC AAG GGC CTC TTC TCT ATC CCT C) and DDX3D3 F-Xh (CTC GAG CCA CCA TGC ACC AGT TCC GCT CAG GAA AAA G) were used, respectively. Reporter and internal control plasmids for reporter gene assay are previously described [26].

RNAi

Knockdown of DDX3 was carried out using siRNA, DDX3 siRNA-1: 5′-GAU UCG UAG AAU AGU CGA ACA-3′, siRNA-2: 5′-GGA GUG AUU ACG AUG GCA UUG-3′, siRNA-3: 5′-GCC UCA GAU UCG UAG AAU AGU-3′ and control siRNA: 5′-GGG AAG AUC GGG UUA GAC UUC-3′. Twenty picomoles of each siRNA was transfected into HEK293 cells in 24-well plates with Lipofectamin 2000 according to manufacture's protocol. Knockdown of DDX3 was confirmed 48 h after siRNA transfection. Experiments were repeated twice for confirmation of the results.

Yeast two-hybrid assay

The yeast two-hybrid assay was performed as described previously [27]. The yeast AH109 strain (Clontech, Palo Alto, CA, USA) was transformed using bait (pGBKT7) and prey (pGADT7) plasmids. The transformants were streaked onto plates and incubated for 3–5 days. The IPS-1 CARD vector was constructed by inserting IPS-1 partial fragment encoding from 6 to 136 aa region into pGBKT7 multicloning site. Yeast two-hybrid screening was performed using human lung cDNA libraries. We obtained four independent clones, and one encoded DDX3 partial cDNA. SD-WLH is a yeast synthetic dextrose medium that lacks Trp, Leu and His aa. SD-WLHA lacks adenine in addition to Trp, Leu and His. SD-WL lacks Trp and Leu and thus non-selective plate.

Reporter assay

HEK293 cells (4×10^4 cells/well) cultured in 24-well plates were transfected with the expression vectors for IPS-1, DDX3 or empty vector together with the reporter plasmid (100 ng/well) and an internal control vector, phRL-TK (Promega) (2.5 ng/well) using FuGENE (Roche) as described previously [28]. The p-125 luc reporter containing the human IFN-β promoter region (−125 to +19) was provided by Dr. T. Taniguchi (University of Tokyo, Tokyo, Japan). The total amount of DNA (500 ng/well) was kept constant by adding empty vector. After 24 h, cells were lysed in lysis buffer (Promega), and the *Firefly* and *Renella* luciferase activities were determined using a dual-luciferase reporter assay kit (Promega). The *Firefly* luciferase activity was normalized by *Renella* luciferase activity and is expressed as the fold stimulation relative to the activity in vector-transfected cells. Experiments were performed three times in duplicate (unless otherwise indicated in the legends).

PolyI:C stimulation

PolyI:C was purchased from GE Healthcare company, and solved in milliQ water. For polyI:C treatment, polyI:C (50 μg/mL) was mixed with DEAE-dextran (0.5 mg/mL) (Sigma) in the culture medium, and the cell culture supernatant was replaced with the medium containing polyI:C and DEAE-dextran. Using DEAE-dextran, polyI:C is incorporated into the cytoplasm to activate RIG-I/MDA5.

Virus preparation and infection

VSV Indiana strain or poliovirus type 1 Mahoney strain were used for virus assay. Vero derived cell (Vero-SLAM) was used for propagation and plaque assay for VSV indiana strain or poliovirus type 1 Mahoney strain. HEK293 cells were infected with viruses at MOI = 0.001 in a 24-well plate. The virus titers of culture media at indicated hours post infection in the figures were determined by plaque assay using Vero-SLAM cells. In some experiments that require rapid virus propagation, high MOI ($0.1 \sim 1$) was used for infection.

Immunoprecipitation

HEK293FT cells were transfected in a 6-well plate with plasmids encoding DDX3, IPS-1, RIG-I or MDA5 as indicated in the figures. Twenty-four hours after tranfection, the total cell lysate was prepared by lysis buffer (20 mM Tris-HCl (pH 7.5) containing 125 mM NaCl, 1 mM EDTA, 10% glycerol, 1% NP-40, 30 mM NaF, 5 mM Na3Vo4, 20 mM IAA and 2 mM PMSF), and the protein was immunoprecipitated with anti-HA polyclonal (Sigma) or anti-FLAG M2 mAb (Sigma). The precipitated samples were resolved on SDS-PAGE, blotted onto a nitrocellulose sheet and stained with anti-HA (HA1.1) monoclonal (Sigma), anti-HA polyclonal or anti-FLAG M2 mAb.

Confocal analysis

HeLa cells were plated onto cover glass in a 24-well plate. In the following day, cells were transfected with indicated plasmids using Fugene HD (Roch). The amount of DNA was kept constant by adding empty vector. After 24 h, cells were fixed with 3% of paraformaldehyde in PBS for 30 min, and then permeabilized with PBS containing 0.2% of Triton

X-100 for 15 min. For the polyI:C stimulation, 100 ng of polyI:C were transfected into HeLa cell in 24-well plates together with IPS-1 or DDX3 expressing vectors, and 24 h after the transfection, the cells were fixed and stained for confocal microscopic analysis. Permeabilized cells were blocked with PBS containing 1% BSA and were labeled with anti-Flag M2 mAb (Sigma), anti-HA polyclonal Ab (Sigma) or Mitotracker in 1% BSA/PBS for 1 h at room temperature. The cells were then washed with 1% BSA/PBS and treated for 30 min at room temperature with Alexa-conjugated Ab (Molecular Probes). Thereafter, micro-cover glass was mounted onto slide glass using PBS containing 2.3% DABCO and 50% of glycerol. The stained cells were visualized at × 60 magnification under a FLUOVIEW (Olympus, Tokyo, Japan).

Acknowledgements: The authors thank Dr. M. Sasai, Dr. T. Ebihara, Dr. K. Funami, Dr. A. Matsuo, Dr. A. Ishii, Dr. A. Watanabe and Dr. M. Shingai in our laboratory for their critical discussions. This work was supported in part by CREST and Innovation, JST (Japan Science and Technology Corporation), the Program of Founding Research Centers for Emerging and Reemerging Infectious Diseases, MEXT, Sapporo Biocluster "Bio-S," the Knowledge Cluster Initiative of the MEXT, Grants-in-Aid from the Ministry of Education, Science, and Culture (Specified Project for Advanced Research) and the Ministry of Health, Labor, and Welfare of Japan, Mitsubishi Foundation, Mochida Foundation, NorthTec Foundation and Takeda Foundation.

Conflict of interest: The authors declare no financial or commercial conflict of interest.

References

1 **Kato, H., Takeuchi, O., Sato, S., Yoneyama, M., Yamamoto, M., Matsui, K., Uematsu, S. *et al.***, Differential roles of MDA5 and RIG-I helicases in the recognition of RNA viruses. *Nature* 2006. **441**: 101–105.

2 **Gitlin, L., Barchet, W., Gilfillan, S., Cella, M., Beutler, B., Flavell, R. A., Diamond, M. S. *et al.***, Essential role of mda-5 in type I IFN responses to polyriboinosinic:polyribocytidylic acid and encephalomyocarditis picornavirus. *Proc. Natl. Acad. Sci. USA* 2006. **103**: 8459–8464.

3 **Yoneyama, M., Kikuchi, M., Natsukawa, T., Shinobu, N., Imaizumi, T., Miyagishi, M., Taira, K. *et al.***, The RNA helicase RIG-I has an essential function in double-stranded RNA-induced innate antiviral responses. *Nat. Immunol.* 2004. **5**: 730–737.

4 **Kawai, T., Takahashi, K., Sato, S., Coban, C., Kumar, H., Kato, H., Ishii, K. J. *et al.***, IPS-1, an adaptor triggering RIG-I- and Mda5-mediated type I interferon induction. *Nat. Immunol.* 2005. **6**: 981–988.

5 **Meylan, E., Curran, J., Hofmann, K., Moradpour, D., Binder, M., Bartenschlager, R. and Tschopp, J.**, Cardif is an adaptor protein in the RIG-I antiviral pathway and is targeted by hepatitis C virus. *Nature* 2005. **437**: 1167–1172.

6 **Seth, R. B., Sun, L., Ea, C. K. and Chen, Z. J.**, Identification and characterization of MAVS, a mitochondrial antiviral signaling protein that activates NF-kappaB and IRF 3. *Cell* 2005. **122**: 669–682.

7 **Xu, L. G., Wang, Y. Y., Han, K. J., Li, L. Y., Zhai, Z. and Shu, H. B.**, VISA is an adapter protein required for virus-triggered IFN-beta signaling. *Mol. Cell* 2005. **19**: 727–740.

8 **Sasai, M., Matsumoto, M. and Seya, T.**, The kinase complex responsible for IRF-3-mediated IFN-beta production in myeloid dendritic cells (mDC). *J. Biochem.* 2006. **139**: 171–175.

9 **Ryzhakov, G. and Randow, F.**, SINTBAD, a novel component of innate antiviral immunity, shares a TBK1-binding domain with NAP1 and TANK. *EMBO J.* 2007. **26**: 3180–3190.

10 **Sasai, M., Oshiumi, H., Matsumoto, M., Inoue, N., Fujita, F., Nakanishi, M. and Seya, T.**, Cutting Edge: NF-kappaB-activating kinase-associated protein 1 participates in TLR3/Toll-IL-1 homology domain-containing adapter molecule-1-mediated IFN regulatory factor 3 activation. *J. Immunol.* 2005. **174**: 27–30.

11 **Saito, T., Hirai, R., Loo, Y. M., Owen, D., Johnson, C. L., Sinha, S. C., Akira, S. *et al.***, Regulation of innate antiviral defenses through a shared repressor domain in RIG-I and LGP2. *Proc. Natl. Acad. Sci. USA* 2007. **104**: 582–587.

12 **Hornung, V., Ellegast, J., Kim, S., Brzozka, K., Jung, A., Kato, H., Poeck, H. *et al.***, 5′-Triphosphate RNA is the ligand for RIG-I. *Science* 2006. **314**: 994–997.

13 **Franca, R., Belfiore, A., Spadari, S. and Maga, G.**, Human DEAD-box ATPase DDX3 shows a relaxed nucleoside substrate specificity. *Proteins* 2007. **67**: 1128–1137.

14 **Yedavalli, V. S., Neuveut, C., Chi, Y. H., Kleiman, L. and Jeang, K. T.**, Requirement of DDX3 DEAD box RNA helicase for HIV-1 Rev-RRE export function. *Cell* 2004. **119**: 381–392.

15 **Kravchenko, V. V., Mathison, J. C., Schwamborn, K., Mercurio, F. and Ulevitch, R. J.**, IKKi/IKKepsilon plays a key role in integrating signals induced by pro-inflammatory stimuli. *J. Biol. Chem.* 2003. **278**: 26612–26619.

16 **Soulat, D., Bürckstümmer, T., Westermayer, S., Goncalves, A., Bauch, A., Stefanovic, A., Hantschel, O. *et al.***, The DEAD-box helicase DDX3X is a critical component of the TANK-binding kinase 1-dependent innate immune response. *EMBO J.* 2008. **27**: 2135–2146.

17 **Venkataraman, T., Valdes, M., Elsby, R., Kakuta, S., Caceres, G., Saijo, S., Iwakura, Y. *et al.***, Loss of DExD/H box RNA helicase LGP2 manifests disparate antiviral responses. *J. Immunol.* 2007. **178**: 6444–6455.

18 **Schroder, M., Baran, M. and Bowie, A. G.**, Viral targeting of DEAD box protein 3 reveals its role in TBK1/IKKepsilon-mediated IRF activation. *EMBO J.* 2008. **27**: 2147–2157.

19 **Gack, M. U., Shin, Y. C., Joo, C. H., Urano, T., Liang, C., Sun, L., Takeuchi, O. *et al.***, TRIM25 RING-finger E3 ubiquitin ligase is essential for RIG-I-mediated antiviral activity. *Nature* 2007. **446**: 916–920.

20 **Oshiumi, H., Matsumoto, M., Hatakeyama, S. and Seya, T.**, Riplet/RNF135, a RING finger protein, ubiquitinates RIG-I to promote interferon-beta induction during the early phase of viral infection. *J. Biol. Chem.* 2009. **284**: 807–817.

21 **Arimoto, K., Takahashi, H., Hishiki, T., Konishi, H., Fujita, T. and Shimotohno, K.**, Negative regulation of the RIG-I signaling by the ubiquitin ligase RNF125. *Proc. Natl. Acad. Sci. USA* 2007. **104**: 7500–7505.

22 **Ariumi, Y., Kuroki, M., Abe, K., Dansako, H., Ikeda, M., Wakita, T. and Kato, N.**, DDX3 DEAD-box RNA helicase is required for hepatitis C virus RNA replication. *J. Virol.* 2007. **81**: 13922–13926.

23 **Chuang, R. Y., Weaver, P. L., Liu, Z. and Chang, T. H.,** Requirement of the DEAD-Box protein ded1p for messenger RNA translation. *Science* 1997. **275**: 1468–1471.

24 **Owsianka, A. M. and Patel, A. H.,** Hepatitis C virus core protein interacts with a human DEAD box protein DDX3. *Virology* 1999. **257**: 330–340.

25 **Mamiya, N. and Worman, H. J.,** Hepatitis C virus core protein binds to a DEAD box RNA helicase. *J. Biol. Chem.* 1999. **274**: 15751–15756.

26 **Sasai, M., Shingai, M., Funami, K., Yoneyama, M., Fujita, T., Matsumoto, M. and Seya, T.,** NAK-associated protein 1 participates in both the TLR3 and the cytoplasmic pathways in type I IFN induction. *J. Immunol.* 2006. **177**: 8676–8683.

27 **Oshiumi, H., Matsumoto, M., Funami, K., Akazawa, T. and Seya, T.,** TICAM-1, an adaptor molecule that participates in Toll-like receptor 3-mediated interferon-beta induction. *Nat. Immunol.* 2003. **4**: 161–167.

28 **Matsumoto, M., Funami, K., Tanabe, M., Oshiumi, H., Shingai, M., Seto, Y., Yamamoto, A. *et al.*,** Subcellular localization of Toll-like receptor 3 in human dendritic cells. *J. Immunol.* 2003. **171**: 3154–3162.

Abbreviations: **CARD:** caspase recruitment domain · **DEAD:** Asp-Glu-Ala-Asp · **DDX3:** DEAD/H BOX 3 · **IKKε:** I-kappa-B kinase ε · **IRF-3:** IFN regulatory factor-3 · **IP:** immunoprecipitation · **IPS-1:** IFN-β promoter stimulator-1 · **MDA5:** melanoma differentiation-associated gene 5 · **RIG-I:** retinoic acid inducible gene-I · **RLR:** RIG-I-like receptor · **TBK1:** TANK-binding kinase 1 · **VSV:** vesicular stomatitis virus

Full correspondence: Dr. Tsukasa Seya, Department of Microbiology and Immunology, Graduate School of Medicine, Hokkaido University, Kita-ku, Sapporo 060-8638, Japan
Fax: +81-11-706-7866
e-mail: seya-tu@pop.med.hokudai.ac.jp

See accompanying Commentary:
http://dx.doi.org/10.1002/eji.201040447

Received: 30/11/2009
Revised: 8/1/2010
Accepted: 19/1/2010
Accepted article online: 1/2/2010

G Model
DCI1419 1–11
ARTICLE IN PRESS

Developmental and Comparative Immunology xxx (2010) xxx–xxx

Contents lists available at ScienceDirect

Developmental and Comparative Immunology

journal homepage: www.elsevier.com/locate/dci

Phylogenetic and expression analysis of lamprey toll-like receptors

Jun Kasamatsu[a], Hiroyuki Oshiumi[a], Misako Matsumoto[a], Masanori Kasahara[b], Tsukasa Seya[a,*]

[a] Department of Microbiology and Immunology, Graduate School of Medicine, Hokkaido University, Kita-ku, Sapporo 060-8638, Japan
[b] Department of Pathology, Graduate School of Medicine, Hokkaido University, Kita-ku, Sapporo 060-8638, Japan

ARTICLE INFO

Article history:
Received 30 October 2009
Received in revised form 17 March 2010
Accepted 17 March 2010
Available online xxx

Keywords:
Toll-like receptor
Lamprey
Evolution
Phylogeny
Interferon
Innate immunity

ABSTRACT

Toll-like receptors (TLRs) have been identified as pivotal sensors recognizing microbial pattern molecules in vertebrates. Whole genome analysis of the teleost *Takifugu rubripes* supports the existence of a fundamental family of *TLR* genes in fish. However, the role of the innate immune system in the context of raising acquired immunity in jawless fish remains unclear. In this study, we annotated 16 lamprey *TLR* genes predicted from the latest genome assembly of lamprey on the basis of homology, and identified their cDNAs from Japanese lamprey, *Lethenteron japonicum*. Phylogenetic analyses indicated that the repertoire of lamprey TLRs consisted of both fish (F)- and mammalian (M)-type TLRs, and it was also demonstrated that lamprey TLRs are constitutively expressed in various organs. Our results suggest that lampreys protect against microorganisms using the innate system consisting of a similar set of M- and F-type TLRs, despite possessing a unique acquired immune system. In addition, *type I interferon* (*IFN*), *interferon regulatory factor* (*IRF*)*-3*, and *IRF7* were not identified in the lamprey genome although TLR adaptor and signal transduction genes were highly conserved upstream of (IRF)-3/7 and type I IFN in most vertebrates. This is the first report to describe the TLR repertoire and IFN system in one of the most primitive vertebrates, the lamprey.

1. Introduction

Many pathogens possess their own genomes that can change the nature of the host, while vertebrates defend against microbial invasion using sophisticated microbial recognition systems. The representative recognition systems for signaling the presence of invading pathogens are known as innate and acquired immunity. In jawed vertebrates, including mammals, these systems have been characterized at the molecular level, with details of the acquired immune system having first emerged from ancient cartilaginous fish (Flajnik and Kasahara, 2001; Litman et al., 1999). The acquired immune system is characterized by the actions of highly variable peptide-antigen receptors, such as immunoglobulins and T-cell receptors. Recent progress on the study of the innate immune system, involving dendritic cells (DCs) and pattern-recognition receptors (PRRs), has revealed that its activation precedes the acquired immune system. PRRs are now a focus of study due to recent elucidation of the ligand properties of toll-like receptors (TLRs) and TLR-mediated DC maturation. Accumulating evidence regarding TLR-mediated DC maturation has helped us solidify the current understanding that TLRs facilitate driving effector cells by maturation of antigen (Ag)-presenting DCs. Accordingly, Ags determine the object toward which immune cells are proliferated whereas microbial patterns determine which effectors are selected for immunological output (Seya and Matsumoto, 2009).

Recent findings have indicated that lamprey possesses a unique acquired immune system involving variable lymphocyte receptors (VLRs) and the lymphoid system (Pancer and Cooper, 2006). In agnathans, which includes lamprey and hagfish, clonally diversed receptors are generated by the assembly of genes for VLRs, which are comprised of leucine-rich repeat (LRR) subunits similar to TLRs. The variable VLR gene products consist of soluble forms and GPI-anchored membrane forms similar to antibodies and antigen receptors (Pancer and Cooper, 2006). However, no relationship between lamprey TLRs and VLR-based acquired system has yet been reported.

TLRs with similar host-defense functions to Drosophila toll protein (Lemaitre et al., 1996) have been identified in mammals (Medzhitov et al., 1997). TLR is a type-1 membrane protein consisting of an LRR extracellular domain, a transmembrane domain, and a C-terminal toll/IL-1 receptor homology domain (TIR). TLRs recognize pathogen-associated molecular patterns (PAMPs), which are characteristic of microbial structures, and induce antimicrobial responses (Takeda et al., 2003). In the human genome, 10 TLR members have been indentified and their functions determined from analyses of TLR-deficient mice (Takeda et al., 2003): the TLR2 subfamily recognizes bacterial cell wall peptidoglycan and acylated lipopeptides, TLR4 recognizes Gram-negative bacterial lipopolysaccharides, TLR5 recognizes bacterial flagellin, while TLR3, 7, 8, and 9 recognize microbial nucleic acids.

* Corresponding author. Tel.: +81 11 7065073; fax: +81 11 7067866.
E-mail address: seya-tu@pop.med.hokudai.ac.jp (T. Seya).

0145-305X/$ – see front matter © 2010 Elsevier Ltd. All rights reserved.
doi:10.1016/j.dci.2010.03.004

Please cite this article in press as: Kasamatsu, J., et al., Phylogenetic and expression analysis of lamprey toll-like receptors. Dev Comp Immunol (2010), doi:10.1016/j.dci.2010.03.004

Mouse TLR stimulation results in signal through one of five adaptor proteins (MyD88, TIRAP/MAL, TICAM-1, TICAM-2 and SARM) (Liew et al., 2005). All TLRs with the exception of TLR3, can signal through the adaptor molecule MyD88. MyD88 recruits members of the interleukin-1 receptor-associated kinase (IRAK) family which in turn activate the key ubiquitin E3 ligase, tumour necrosis factor receptor-associated factors (TRAFs) and transforming growth factor-β (TGF-β)-activating kinase (TAK1), leading to the activation of the transcription factor NF-κB (Takeda et al., 2003; Liew et al., 2005). The activated NF-κB is translocated to the nucleus and induces expression of inflammatory cytokine genes such as IL-1β and IL-6. In contrast, TLR3 recruits the adaptor molecule TICAM-1, leading to activation of interferon (IFN) regulatory factor-3 (IRF-3) and induces an antiviral response through expression of type I IFN and IFN-inducible genes (Liew et al., 2005; Seya et al., 2009). Although the MyD88 pathway is conserved in a wide range of vertebrates, whether or not the TICAM-1 pathway is conserved in lower vertebrates is still controversial (Seya et al., 2009).

Advances in whole genome sequencing and annotation have enabled the identification of TLRs from several vertebrates, including osteichthyes fish (fugu) (Oshiumi et al., 2003a), amphibian, (frog) (Ishii et al., 2007a), bird (chicken) (Boyd et al., 2007) and mammals (human and mouse). Comparison of the TLR families across the vertebrate species has revealed that water-living vertebrates possess TLR14, 21 and 22, in addition to the mammalian-type TLRs (Roach et al., 2005; Oshiumi et al., 2008). Our earlier studies speculate that the TLR repertoire was established during evolution in a species-specific manner in jawed vertebrates depending upon their living environment, such as water or land (Oshiumi et al., 2003a; Ishii et al., 2007a; Higuchi et al., 2008). On the other hand, some invertebrates, the sea urchin and amphioxus, possess a large number of TLRs (Hibino et al., 2006; Rast et al., 2006; Holland et al., 2008; Huang et al., 2008), while *Ciona intestinalis* has only 2 functional TLRs (Irvine et al., 2002) from their genome projects. Thus, what happens in the TLR system lamprey is of interest in tems of the evolution.

Our previous study identified two lamprey TLRs, named laTLR14a and 14b, by PCR-based cloning using sequences of TLR2 from various animals (Ishii et al., 2007b). However, no conclusive identification of TLRs in the lamprey genome had been made until recently. Here, we surveyed the amino acid sequences of predicted TIR-containing proteins from the latest *Petromyzon marinus* genome database (Pre-Ensemble Lamprey Genome Browser) and NCBI trace archive, and the predicted protein sequences of the lamprey TLRs and their respective TIR domains were subjected to comparative analyses using the NCBI non-redundant protein database and BLASTP search. Ultimately, we determined the repertoire of predicted lamprey TLRs in this report.

2. Materials and methods

2.1. Identification of TLR and innate immune genes in the P. marinus genome

Sea lamprey (*P. marinus*) EST sequences were retrieved from the NCBI trace archive (http://www.ncbi.nlm.nih.gov/Traces/trace.cgi) and a private database was constructed using the GENETYX-PDB program package (version 5, GENETYX Corporation). This database, and the EST database from NCBI, was searched with the TBLASTN program using putative amino acid sequences of lamprey TLRs and innate immunity genes from previously annotated human and fugu TLRs (Oshiumi et al., 2003a). The genes that were not found by these analyses were searched with the TBLASTN program using the Pre Ensembl genome browser (http://pre.ensembl.org/Petromyzon_marinus/Info/Index).

Domain structures of the *P. marinus* TLR (pmTLR) proteins were analyzed by the SMART program (http://smart.embl-heidelberg.de). An unrooted phylogenetic tree based on the amino acid sequences was constructed by the Neighbor-joining (NJ) method in the ClustalX version 2 program (Larkin et al., 2007) and the MEGA version 4 program (Tamura et al., 2007). The distance matrix was obtained by calculating p-distances for all pairs of sequences. Sites containing gaps were excluded from the analysis using the pairwise deletion option. The reliability of branching patterns was assessed by bootstrap analysis (1000 replications). The accession numbers of the sequences used for gene-searching and phylogenetic analysis are listed in Table 1.

2.2. Expression analysis of TLRs and their adaptor genes in Lethenteron japonicum

An adult Japanese lamprey (*L. japonicum*) was used to analyze the differential expression of *L. japonicum* TLR (LjTLR) mRNAs in various tissues. This is because 1. we have no sea lamprey (*P. marinus*) in Japan, and 2. *L. japonicum* belongs to Petromyzoninae, the same family as *P. marinus*. Although we have no genome database of *L. japonicum*, it is expected that the genome of *L. japonicum* has highly homologous to that of *P. marinus*. For the analysis, 100 mg of each frozen tissue was homogenized and total RNA was extracted using an RNeasy mini kit (Qiagen). One μg of total RNA was treated with RQ1 RNase-free DNase (Promega) and reverse transcribed with M-MLV RTase (Promega) using random primers. For amplification of TLR and innate immunity gene cDNA fragments, PCR reactions were typically performed by denaturation at 94 °C for 2 min followed by 30–45 cycles of 94 °C for 30 s, 50–60 °C for 30 s, and extension at 72 °C for 30 s using Ex-Taq polymerase (Takara) (each primer set and PCR condition are listed in Table 3). The size of the cDNA fragments was confirmed using electrophoresis with 3% agarose gels. All amplicons were cloned into vectors using the pGEM®-T Easy Vector System (Promega) or TOPO TA Cloning System (Invitrogen) and their sequences were determined using an automated sequencer.

2.3. Lamprey blood cell stimulation

Blood cells were separately collected from each individual of lampreys (*L. japonicum*) one day after arrival. Peripheral blood leukocytes (PBLs) were drawn from the severed tails of fish into PBS containing 30 mM EDTA. Buffy-coat leukocytes were collected by centrifugation for 30 min at 1500 rpm. The cells were incubated with polyI:C and heat killed *Escherichia coli* (*E. coli*) as indicated in Fig. 5 and allowed to stand for 3 h or 6 h. Then, total RNA was extracted using an RNeasy mini kit (Qiagen). RT-PCR was performed as described above.

3. Results

3.1. Identification of TLRs in the lamprey genome

A typical TLR consists of multiple LRRs at the N-terminus, a transmembrane domain, and a TIR domain in the C-terminus. The TIR domain is important for signal transduction and recruits adaptor molecules which also contain a TIR domain (Takeda et al., 2003). We attempted to identify genes encoding TLRs and their adaptors from the EST and genome databases of sea lamprey (Pre-Ensemble Lamprey Genome Browser) using human TLR1-10, TICAM-1, MyD88, TICAM-2, TIRAP, and SARM (Liew et al., 2005), mouse TLR12 and 13, and Fugu TLR21 and 22 (Ishii et al., 2007a) as query sequences. Ultimately, 20 genes predicted to encode typical TIR domains were identified (Table 2), of which 16 harbored multiple LRRs and were therefore defined as lamprey TLR proteins

Please cite this article in press as: Kasamatsu, J., et al., Phylogenetic and expression analysis of lamprey toll-like receptors. Dev Comp Immunol (2010), doi:10.1016/j.dci.2010.03.004